

YkgM and YkgO maintain translation by replacing their paralogs, zinc-binding ribosomal proteins L31 and L36, with identical activities

Masami Ueta  | Chieko Wada  | Akira Wada 

Yoshida Biological Laboratory, Kyoto, Japan

Correspondence

Chieko Wada and Akira Wada,
Yoshida Biological Laboratory, 11-1
Takehanasotoda-cho, Yamashina-ku, Kyoto
607-8081, Japan.
Emails: chiewada6@gmail.com (C. W.);
awada@yoshidabio.co.jp (A. W.)

Abstract

When a cell is zinc-deficient, *ykgM* and *ykgO*, which encode paralogs of the zinc-binding ribosomal proteins L31 and L36, are expressed from the *ykgM* operon, which is ordinarily held inactive by the Zur repressor. In ribosomes lacking L31, ribosomal subunit association is weakened, resulting in reduced in vitro translation and the deletion mutants of *rpmE*, the gene encoding L31, forming small colonies. We isolated four suppressor mutants of $\Delta rpmE$ that formed normal colonies. All four mutation sites were located in *zur*, and ribosomes of *zur* mutant cells contained one copy of YkgM and had translational activities equivalent to those of ribosomes containing L31. L36 is highly conserved among bacteria, chloroplast and mitochondria. Analysis of a deletion mutant of *rpmJ*, which encodes L36, suggested that L36 is involved in late assembly of the 50S particle, in vitro translation and cell growth. In *zur* mutant cells lacking *rpmJ*, the paralog YkgO was expressed and took over the functions of L36. *zur* mutant cells contained four types of ribosomes containing combinations of L31 or YkgM, and L36 or YkgO. Copy numbers of L31 and YkgM, and L36 and YkgO, summed to 1, indicating that each paralog pair shares a binding site.

KEYWORDS

ribosomal protein L31, ribosomal protein L36, ribosome assembly, translational activity, YkgM, *ykgM* operon, YkgO, zinc-binding ribosomal protein, Zur

1 | INTRODUCTION

The ribosome is an essential cellular component, widely conserved among organisms, which is responsible for translating genetic information from the nucleotide sequence of mRNA to the amino acid sequence of a protein. In bacteria, small (30S) and large (50S) subunits associate and form the 70S ribosomal particle, which is active in translation. In *Escherichia coli*, the 30S subunit consists of 16S rRNA and 21 ribosomal proteins (r-proteins), and the 50S subunit contains 23S rRNA, 5S rRNA and 33 r-proteins (Kaltschmidt &

Wittmann, 1970; Wada, 1986a, 1986b; Wada & Sako, 1987). In addition to the r-proteins identified by Kaltschmidt and Wittmann (1970), L35 (A), L36 (B) and full-length (intact) L31 (C) were discovered using radical-free and highly reducing two-dimensional-polyacrylamide gel electrophoresis (RFHR 2D-PAGE) (Wada, 1986a,b; Wada & Sako, 1987). All three of the newly detected r-proteins are widely conserved in bacterial ribosomes. Thus, 54 r-proteins are now recognized to constitute the ribosome.

We found that the eight C-terminal amino acids of L31 are artificially cleaved during ribosome preparation by outer

membrane protein protease 7 (encoded by *ompT*), leading to the formation of a short form of L31 (Ueta, Wada, Bessho, Maeda, & Wada, 2017). Initially, this short L31 was defined as L31 itself (Brosius, 1978). We investigated the function of L31 using three ribosomal populations: (a) ribosomes containing both intact and short L31 obtained from wild-type cells; (b) ribosomes containing just intact L31, prepared from $\Delta ompT$ cells; and (c) ribosomes containing no L31, prepared from $\Delta rpmE$ cells. We found that L31 plays important roles in 70S formation by promoting association of the 30S and 50S subunits, and that the eight C-terminal amino acids of L31 are involved in subunit association. The translational activities of ribosomes prepared from $\Delta rpmE$ cells were 40% lower than those of *ompT*-mutant ribosomes (wild type), indicating that intact L31 is involved in translation in vitro. Structural analysis by cryo-electron microscopy (cryo-EM) showed that the L31 protein spans the 30S and 50S subunits (Agirrezabal et al., 2012; Fischer et al., 2015). This placement is reasonable for the roles of L31 in 30S and 50S subunit association and translation activity (Ueta et al., 2017).

In the stationary phase, *E. coli* cells form dimers of 70S (100S ribosomes) via an interaction with ribosome modulation factor (RMF) (Wada, Igarashi, Yoshimura, Aimoto, & Ishihama, 1995; Wada, Yamazaki, Fujita, & Ishihama, 1990) and hibernation promoting factor (HPF), both of which are expressed specifically under stressful conditions (Izutsu, Wada, & Wada, 2001; Maki, Yoshida, & Wada, 2000; Shimada, Yoshida, & Ishihama, 2013; Ueta et al., 2005, 2008; Wada, 1998; Yoshida & Wada, 2014). The 100S ribosome lacks translational activity because RMF binds near the peptidyl transferase center and peptide exit tunnel (Yoshida et al., 2002; Yoshida, Yamamoto, Uchiyumi, & Wada, 2004). Cryo-EM showed that the structure of the 100S ribosome relies on interactions between the S2, S3, S4 and S5 proteins of the 30S subunit, and lacks tRNA and mRNA (Kato et al., 2010; Ortiz et al., 2010). Ribosomes lacking L31 failed to form the 100S ribosome in the stationary phase, consistent with the idea that L31 is also involved in 100S formation in addition to 30S and 50S subunit association and translation activity (Ueta et al., 2017). The 100S particle is widely conserved in bacteria and probably serves to negatively regulate translational activity via dimerization of active 70S (Ueta et al., 2013). Furthermore, L31 forms together with S13 and L5 Bridge B1b, which connects the 50S and 30S subunits and plays a crucial role in ribosome dynamics due to rotational movements of the subunits during translation process and is important for determining translational fidelity and stabilizing subunit association (Chadani et al., 2017; Fischer et al., 2015; Lilleorg et al., 2019; Liu & Fredrick, 2016; Shasmal, Chakraborty, & Sengupta, 2010; Ueta et al., 2017).

Zinc is an essential metal ion in all organisms and a necessary component of many proteins involved in fundamental basic cellular processes. Several r-proteins contain zinc;

proteomic studies have shown that *E. coli* ribosomal proteins L2, L13, S2, S15, S16 and S17 can bind Zn (II) (Katayama, Tsujii, Wada, Nishino, & Ishihama, 2002). X-ray absorption fine structure (EXAFS) studies showed that the *E. coli* 70S ribosome binds eight equivalents of Zn (II) (S2, S15, S16, S17, L2, L13, L31 and L36) (Hensley, Tierney, & Crowder, 2011). However, only two *E. coli* r-proteins, L31 and L36, contain a predicted Zn (II)-ribbon motif (Makarova, Ponomarev, & Koonin, 2001; Panina, Mironov, & Gelfand, 2003); the Zn (II)-binding sites in L31 (Hensley et al., 2012) and L36 (Lilleorg et al., 2019) were showed by cryo-EM and X-ray crystallography, respectively.

The *E. coli* genome contains two L31 genes: *rpmE*, which encodes L31 (a Zn (II)-responsive gene), and *ykgM* (is also called *rpmE2*), which encodes the L31 paralog YkgM. In medium containing zinc, only *rpmE* is expressed. Under zinc deficiency, transcription of the operon containing *ykgM* is induced by inactivation of the transcriptional regulator Zur (zinc-dependent regulator), which represses the promoter of the operon and regulates gene expression in response to zinc levels (Graham et al., 2009; Hemm et al., 2010). YkgM (87 amino acids, MW 9,920.20 Da, pI 9.30) is 17 amino acids longer than L31 (70 amino acid, MW 7,871.06 Da, pI 9.46), but the two proteins have very similar sequences in their N-terminal and C-terminal regions. L31 has one Zn-binding motif (CxxC: C16-S17-C18-Xn-C37-S38-K39-C40), whereas YkgM has none. Moreover, YkgM lacks the cleavage site recognized by protease 7 (K↓R), which is present in L31 (Figure S1(1)).

L36, the other zinc-binding r-protein in *E. coli*, binds to one Zn (II) via Cys11, Cys14, Cys27 and His33. The *ykgO* gene is a paralog of *rpmJ*. YkgO (46 amino acids, MW5463.12Da, pI 11.40) is eight amino acids longer than L36 (38 amino acids, MW 4,364.33Da, pI 10.69), but the two proteins are otherwise very similar (Figure S1(2)). *ykgM* and *ykgO* are contained within the *ykgM-ykgO* operon, whose transcription is inhibited by the Zur repressor. When Zur is inactivated under zinc depletion, the operon is induced, and YkgM and YkgO are expressed.

In addition to the *ykgM-ykgO* operon, the Zur regulon of gamma-proteobacteria includes the *znuABC* cluster of zinc uptake genes; *zint*, which encodes a periplasmic zinc trafficking protein; and the *hlyCABD* operon (Hantke, 2005; Hemm et al., 2010; Li et al., 2009; Panina et al., 2003; Velasco et al., 2018). The 23 bp consensus sequence for Zur-binding sites in gamma-proteobacteria, including *Escherichia coli*, was determined by computational analysis (Panina et al., 2003). Further refinement showed that the sequence recognized by Zur is a 13 bp palindrome with a three-base spacer (RNNNYxxxRNNNY) (Gilston et al., 2014).

We discovered that L36 is a component of the 50S particle (Wada, 1986a, 1986b; Wada & Sako, 1987). L36 is conserved highly in bacteria, mitochondria and chloroplasts

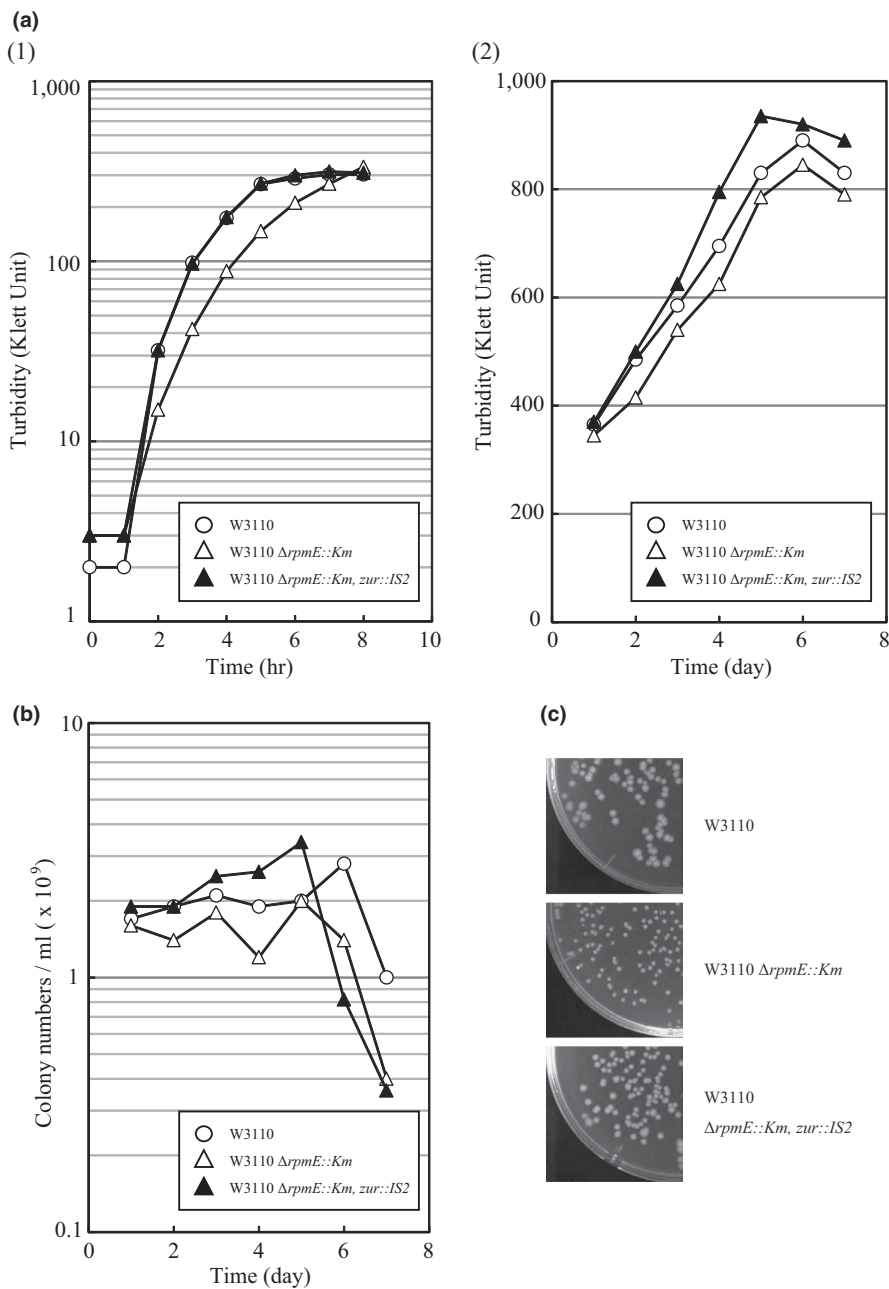


FIGURE 1 Depletion of L31 inhibits bacterial growth in both liquid EP and solid LB media, but *zur* mutation rescues the growth inhibition. (a) W3110 (open circles), W3110 $\Delta rpmE::Km$ (open triangles) and W3110 $\Delta rpmE::Km$ & *zur::IS2* (closed triangles) were cultured in EP medium at 37°C. Cell growth was monitored by measuring turbidity (Klett units). Time scales are 0–8 hr (1) and 1–7 days (2). The vertical axis shows normal logarithmic values for 0–8 hr and a linear scale for 1–7 days. (b) Colony-forming unit (CFU) values of the three strains listed in (a). Cultured cells were sampled every day over 1–7 days of cultivation, and the CFU value was measured. (c) Bacterial colony size on LB solid medium. W3110, W3110 $\Delta rpmE::Km$ and W3110 $\Delta rpmE::Km, zur::IS2$ cells incubated overnight at 37°C in LB medium were spread by diluting the samples as indicated on solid agar plates. The plates were incubated overnight (16–18 hr) at 37°C. Images of the resultant colonies are shown

(Table S3), but it is not present in archaea or the nuclear genome of eukaryotes. Cross-linking studies showed that L36 interacts with 23S rRNA (Urlaub, Kruft, Bischof, Müller, & Wittmann-Liebold, 1995), and chemical protection experiments showed that it plays a significant role in organizing 23S rRNA structure (Maeder & Draper, 2005). 2'-O-methylation of uridine at position 2552 of 23S rRNA by the RlmE methyltransferase promotes association between helices 92 and 71 of 23S rRNA, which together with incorporation of L36 promotes the late steps of 50S ribosomal subunit assembly (Arai et al., 2015). Although *rpmJ* is nonessential, deletion of the gene results in a temperature-sensitive growth defect (Maeder & Draper, 2005).

Both L31 and L36 of *E. coli* are zinc-binding r-protein. Under zinc-limited conditions, YkgM and YkgO are expressed due to inactivation of Zur repressor, and replace their paralogs in the ribosome. In *zur* mutant cells, L31, L36, YkgM and YkgO are all expressed in the logarithmic growth phase, as well as in the stationary phase. The *rpmE zur* double mutant expresses the paralog YkgM, and the *rpmJ zur* double mutant expresses the paralog YkgO from the *ykgM-ykgO* promoter. Previously, however, it was not known whether YkgM and YkgO functionally substitute their paralogs. In this study, we investigated comparatively the functions of L31, YkgM and L36, YkgO using ribosomes prepared from mutant cells.

2 | RESULTS

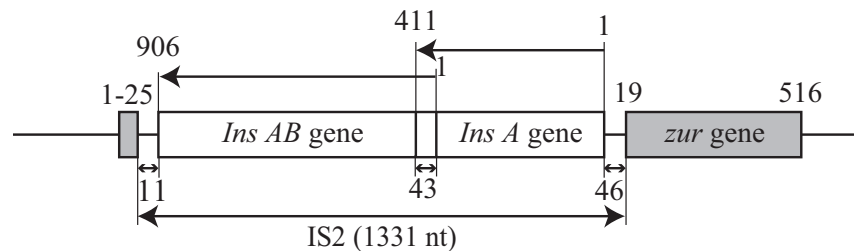
2.1 | $\Delta rpmE$ cells grow slowly and forms small colonies, but the growth defect is suppressed by *zur* mutation

W3110 $\Delta rpmE::Km$ (YB1010) cells, which do not contain ribosomal protein L31, grew more slowly (doubling time [DT], 35–40 min) than the parental strain (DT, 18–20 min) in EP liquid medium and formed small colonies on L-broth agar plates at 37°C [(Figure 1a–c) (Ueta et al., 2017)]. Likewise, BW25113 $\Delta rpmE::Km$ [JW3907-1, Keio collection (Baba et al., 2006)] cells grew more slowly than parental cells (BW25113) (Figure S2A–C). We isolated a total of

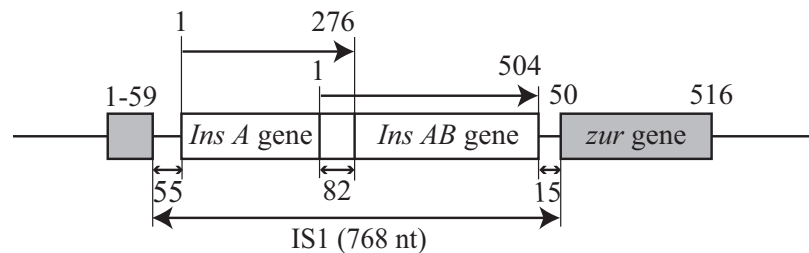
four spontaneous mutants that formed colonies of normal size, three from W3110 $\Delta rpmE::Km$ and one from BW25113 $\Delta rpmE::Km$.

Based on the prediction that these mutations would affect expression of the *zur* gene or the behavior of the Zur protein, we determined the mutation sites by sequencing the *zur*-binding promoter region and *zur* gene itself. All four mutations were located in the *zur* gene. In the three suppressors of W3110 $\Delta rpmE::Km$, the mutation sites in *zur* were an IS2 insertion 25 nt from the 5' end (YB1018), an IS1 insertion 59 nt from the 5' end (YB1024) and the G422A/Gly141Glu point mutation (YB1025) [Figure 2(1),(2),(3)]. The mutation in BW25113 $\Delta rpmE::Km$ was the T200A/Leu67Gln point mutation (YB1022).

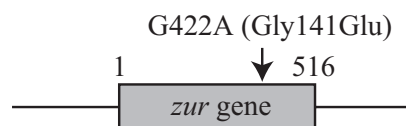
(1) YB1018 (W3110 $\Delta rpmE::Km$ *zur::IS2*)



(2) YB1024 (W3110 $\Delta rpmE::Km$ *zur::IS1*)



(3) YB1025 [W3110 $\Delta rpmE::Km$ *zur* (G422A)]



(4) YB1022 [BW25113 $\Delta rpmE::Km$ *zur* (T200A)]

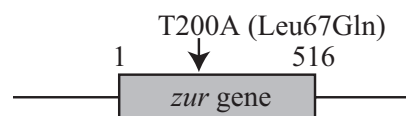


FIGURE 2 The locations of *zur* mutations. The mutation sites of YB1018, YB1024, YB1025 and YB1022 were determined as described in the Section 4

The four mutants grew as well as their original parental strains (W3110 and BW25113) in liquid and solid media in both exponential and stationary phases [Figure 1a(1),(2),b,c; Figure S2A(1),(2),B,C].

2.2 | High-salt-washed ribosomes (HSRs) from W3110 $\Delta rpmE::Km zur::IS2$ mutant cells contain one copy of YkgM in the 50S subunit

When the Zur repressor is inactivated by mutation of *zur*, genes in the *zur* regulon of *E. coli* (*pliG*, *znuABC*, *zinT* and *ykgM-ykgO*) are induced (Gilston et al., 2014; Mikhaylina, Ksibe, Scanlan, & Blindauer, 2018; Patzer & Hantke, 2000). Using the W3110 $\Delta rpmE::Km zur::IS2$ mutant strain, we sought to determine whether the L31 paralog YkgM and L36 paralog YkgO would be incorporated into ribosomes and suppress the *rpmE* mutant phenotype when the *ykgM-ykgO* operon was expressed.

We prepared HSRs from five strains: W3110 (wild type), $\Delta ykgM::Km$ (YB1011), $\Delta rpmE::Km$ (YB1010), $\Delta rpmE \Delta ykgM::Km$ (YB1013) and $\Delta rpmE::Km zur::IS2$ (YB1018). Cells were grown in EP medium at 37°C to exponential phase (Klett units: 50). We then analyzed the r-proteins of each HSR by RFHR 2D-PAGE. Ribosomes of wild-type and $\Delta ykgM::Km$ cells contained equal levels of full-length and short L31 [Figure 3(1)a,b and (2)a,b]. Short L31 is an artificial product generated by protease 7 cleavage during ribosome preparation (Ueta et al., 2017). By contrast, in HSRs of $\Delta rpmE::Km$, neither L31 nor YkgM was detected. Because $\Delta rpmE::Km$ does not express *ykgM* under the growth conditions used in this experiment (EP medium), the r-protein pattern derived from this strain was the same as that in the $\Delta rpmE \Delta ykgM::Km$ strain (YB1013) [Figure 3(3)a,b and (4)a,b].

Ribosomes of BW25113 $\Delta rpmE::Km$ cells, one of the Keio collection strains, contained neither L31 nor YkgM (Figure S3A). Under the growth conditions used for this experiment, zinc was not depleted, so *ykgM* was not expressed despite the lack of L31.

In HSRs of W3110 $\Delta rpmE::Km zur::IS2$ cells, YkgM was present at one copy per ribosome [Figure 3(5)a,b]. HSRs from BW25113 $\Delta rpmE::Km zur$ (T200A) cells also contained one copy of YkgM per ribosome, as did W3110 $\Delta rpmE::Km zur::IS2$ cells (Figure S3A).

We next sought to determine whether YkgM was present in the 50S or 30S subunit. To this end, we prepared 50S and 30S subunits from HSRs of W3110 $\Delta rpmE::Km zur::IS2$ cells and analyzed them by RFHR 2D-PAGE. The results showed that YkgM protein was present in the 50S subunit but not in the 30S subunit (Figure 3c; Figure S3B). Because YkgM does not contain the amino acid sequence cleaved by protease 7 (K↓R), loss of yield due to cleavage during ribosome preparation (Ueta et al., 2017) was avoided, in contrast to the situation for L31 in W3110 wild-type cells.

Together, these results show that the *rpmE* paralog *ykgM* is expressed in *zur* mutant cells irrespective of the presence of zinc and that YkgM is incorporated into ribosomes at one copy per 50S subunit.

2.3 | 50S subunits containing YkgM associate with 30S subunits, forming 70S ribosomes in vivo and in vitro as effectively as 50S subunits containing L31

$\Delta rpmE$ cells contain reduced levels of 70S ribosomes, and correspondingly elevated levels of free 30S and 50S subunits, both in vivo and in vitro, suggesting that L31 promotes the 30S–50S association (Ueta et al., 2017). We investigated whether the L31 paralog YkgM could restore this association in $\Delta rpmE$ cells. For this purpose, four cells (W3110 $\Delta ompT::Km$, $\Delta rpmE::Km$, $\Delta rpmE \Delta ykgM::Km$ and $\Delta rpmE::Km zur::IS2$) were grown in EP medium at 37°C, and the cells were collected in logarithmic growth phase (Klett units: 50) and used to prepare HSRs. To examine subunit association in these HSRs, we analyzed ribosome profiles by sucrose density gradient (SDG) centrifugation under various Mg^{2+} concentrations (2, 3, 5, 6, 8, 10 and 15 mM). After SDG centrifugation in 10 or 15 mM Mg^{2+} , ribosome profiles in all four strains exhibited a main peak corresponding to 70S [Figure 4A(1)–(4)]. After SDG centrifugation in 8, 6 or 5 mM Mg^{2+} , the main 70S peak was still present in $\Delta ompT::Km$. By contrast, in $\Delta rpmE::Km$ and $\Delta rpmE \Delta ykgM::Km$, in 8 mM Mg^{2+} , the 70S peak shifted to a lower S value, and in 5 or 6 mM Mg^{2+} , the magnitude of the 70S peak decreased, and the 30S and 50S peaks grew [Figure 4a(2),(3) compared with Figure 4a(1),(4)]. In 2 mM Mg^{2+} , 70S completely dissociated into 30S and 50S in all four strains [Figure 4a(1)–(4)].

In HSRs of $\Delta ompT::Km$, which carried one copy of intact L31, and those of $\Delta rpmE::Km zur::IS2$, which carried one copy of YkgM, ribosome profiling showed that almost all the ribosomes were present in the 70S form, with very low levels of free ribosomal subunits in 5–15 mM Mg^{2+} . At 3 mM Mg^{2+} , however, 70S shifted to a lower S value [Figure 4a(1),(4)]. HSRs derived from BW25113 $\Delta rpmE::Km zur$ (T200A) cells also recovered association activity relative to $\Delta rpmE::Km$ cells (Figure S4A).

To further examine the association of 30S and 50S in vitro, we cultured the four strains (W3110 $\Delta ompT::Km$, $\Delta rpmE::Km$, $\Delta rpmE \Delta ykgM::Km$ and $\Delta rpmE::Km zur::IS2$) in EP medium at 37°C, collected them in logarithmic growth phase (Klett units: 50) and used them to prepare HSRs. We dissociated the HSRs into 30S and 50S, re-associated them by incubation for 30 min at 37°C and then analyzed the re-associated mixtures by SDG centrifugation in 6 or 15 mM Mg^{2+} . In wild-type HSRs, 70S was observed as the main peak in both 6 and 15 mM Mg^{2+} [Figure 4b(1)]. In $\Delta rpmE::Km$ and

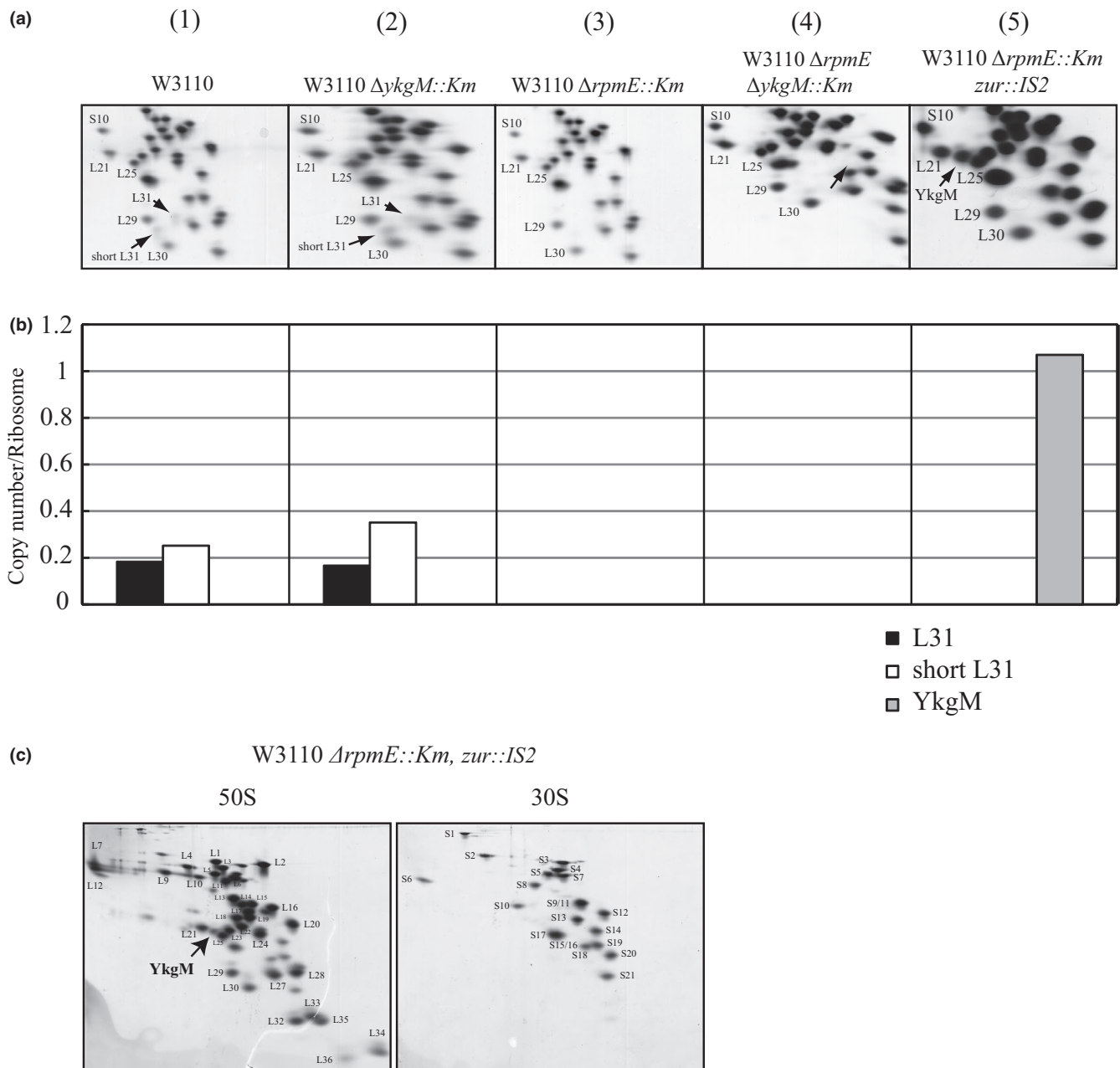


FIGURE 3 Ribosomes prepared from W3110 $\Delta rpmE::Km zur::IS2$ cells each contain one copy of YkgM. (a) W3110 wild-type (1), $\Delta ykgM::Km$ (2), $\Delta rpmE::Km$ (3), $\Delta rpmE \Delta ykgM::Km$ (4) and $\Delta rpmE::Km zur::IS2$ (5) cells were grown at 37°C in EP medium and collected in logarithmic growth phase (Klett units: 50); high-salt-washed ribosomes (HSRs) were prepared. HSR proteins were analyzed by RFHR 2D-PAGE. Gels were stained with CBB. Spots corresponding to r-proteins S10, L21, L25, L29, L30, intact L31, short L31 and YkgM are indicated. (b) Copy numbers of L31 (closed square), short L31 (open square) and YkgM (gray square) are shown. (c) The L31 paralog YkgM is contained in the 50S subunit, not the 30S subunit. W3110 $\Delta rpmE::Km zur::IS2$ cells were grown at 37°C in EP medium and collected in logarithmic growth phase (Klett units: 50). HSRs were suspended in dissociation buffer I and dialyzed against the same buffer overnight. The samples were fractionated by 10%–40% SDG centrifugation in dissociation buffer, and 50S and 30S fractions were collected. Each fraction was analyzed by RFHR 2D-PAGE, and patterns after CBB staining are shown

$\Delta rpmE \Delta ykgM::Km$ cells, 70S was observed in 15 mM Mg^{2+} , whereas in 6 mM, very little 70S was present, and ribosomes with lower S values were detected [Figure 4b(2),(3)]. On the other hand, in the ribosome profile of $\Delta rpmE zur::IS2$ cells (with one copy of YkgM), a prominent 70S peak was observed in both 6 and 15 mM Mg^{2+} [Figure 4b(4)], as in HSRs

from $\Delta ompT::Km$ (with one copy of L31). In HSRs prepared from BW25113 $\Delta rpmE::Km zur$ (T200A) cells, a prominent 70S peak was also observed in 6 mM Mg^{2+} , in contrast to $\Delta rpmE::Km$ cells (Figure S4B).

The in vitro findings correspond with the in vivo results described above and verify that YkgM plays an important role

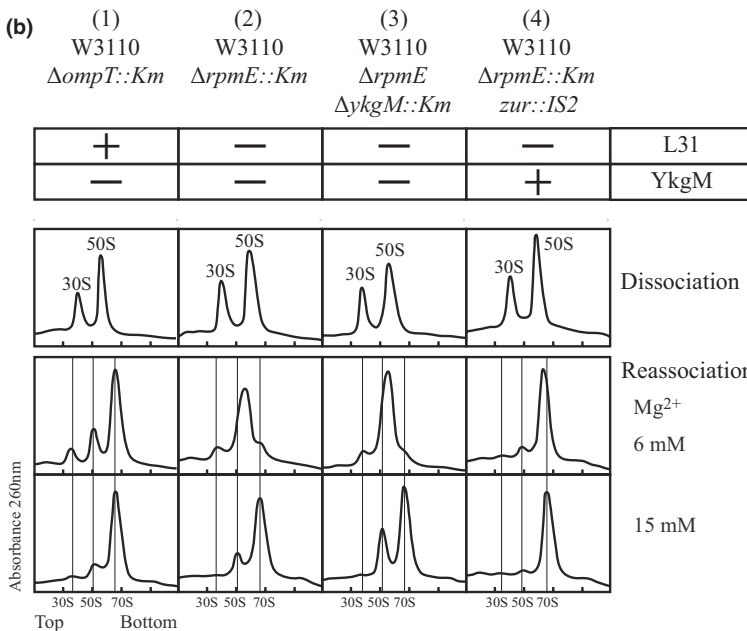
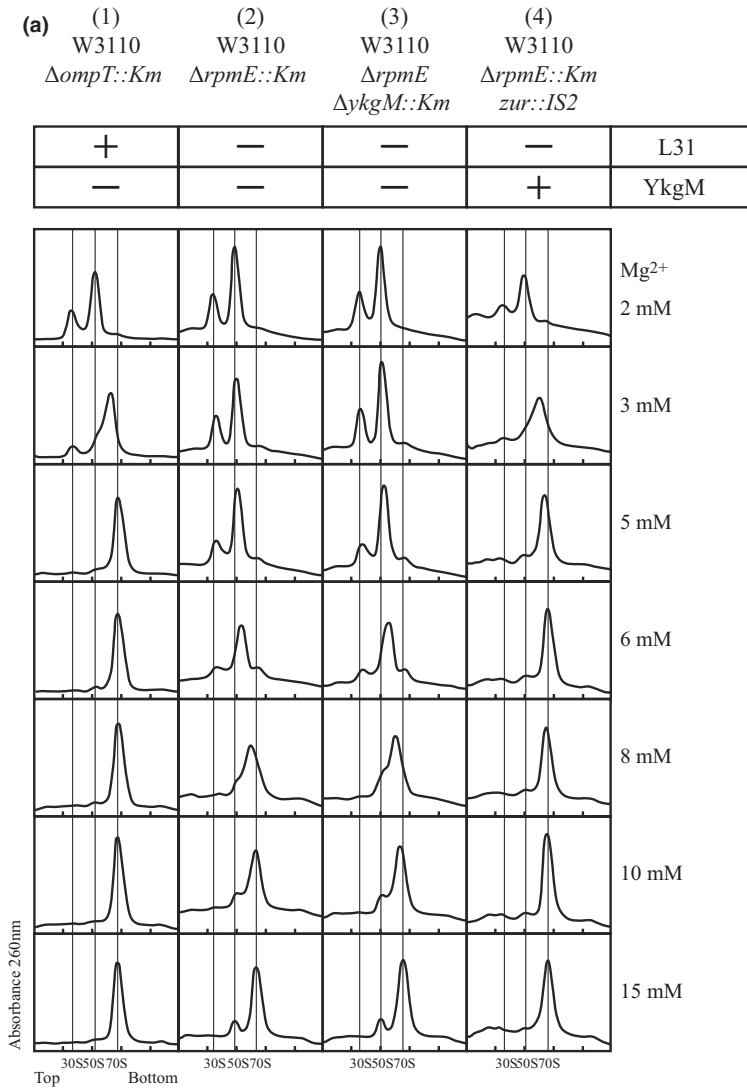


FIGURE 4 (a) High-salt-washed ribosomes (HSRs) without L31 dissociate into 30S and 50S subunits during SDG centrifugation under low Mg^{2+} conditions, but HSRs containing YkgM form 70S. HSRs of W3110 $\Delta ompT::Km$ (1), $\Delta rpmE::Km$ (2), $\Delta rpmE \Delta ykgM::Km$ (3) and $\Delta rpmE::Km \& zur::IS2$ (4) cells were grown at 37°C in EP medium and collected in logarithmic growth phase (Klett units: 50). HSRs were prepared and analyzed by 5%–20% SDG centrifugation at the indicated Mg^{2+} concentrations. The resultant ribosome profiles are shown. (b) Dissociated ribosomes (50S + 30S) containing no L31 form unstable 70S in vitro, but YkgM-containing ribosomes form stable 70S. HSRs were prepared from the following four types: W3110 $\Delta ompT::Km$ (1), $\Delta rpmE::Km$ (2), $\Delta rpmE \Delta ykgM::Km$ (3) and $\Delta rpmE::Km zur::IS2$ (4). HSRs of each strain were dissociated into 30S and 50S subunits. A sample (60 pmol) was layered onto a 5%–20% SDG in dissociation buffer II and centrifuged. The ribosome profiles are shown in the dissociation panels. Dissociated HSRs were incubated at 37°C for 30 min to allow re-association. The samples (60 pmol) were analyzed by 5%–20% SDG centrifugation in 6 or 15 mM Mg^{2+} . The resultant ribosome profiles are shown in the re-association panels

in 30S–50S association to form 70S. The measured properties of these ribosomes were identical to those of $\Delta ompT::Km$, which contained one copy of intact L31 (Figure 4a), suggesting that YkgM binds to the ribosome in place of L31 and functionally substitutes for it.

2.4 | Ribosomes containing YkgM form 100S ribosomes in stationary phase, like ribosomes containing intact L31 protein

In stationary phase, the majority of 70S ribosomes assemble into 100S ribosomes (70S dimer), which do not have translational activity. Formation of 100S is executed by RMF and facilitated by HPF (Maki et al., 2000; Ueta et al., 2005; Wada, 1998; Wada et al., 1990; Yoshida & Wada, 2014). W3110 $\Delta rpmE::Km$ ribosomes, which lack L31, cannot form stable 100S ribosomes in stationary phase (Ueta et al., 2017). Hence, we investigated whether ribosomes carrying YkgM recover the ability to form 100S ribosomes.

For this purpose, we grew three strains (W3110 wild type, $\Delta rpmE::Km$ and $\Delta rpmE::Km zur::IS2$) in EP medium at 37°C and collected the cells after 1 or 3 days of culture. Crude ribosomes (CRs) from the cells were prepared and

analyzed by SDG centrifugation in 5, 8 or 15 mM Mg^{2+} . In CRs of $\Delta rpmE::Km$, which contain neither intact L31 nor YkgM, 100S was observed in 8 and 15 mM Mg^{2+} , but shifted to a lower S value in 5 mM Mg^{2+} . In CRs of $\Delta rpmE::Km zur::IS2$, which contain only YkgM, 100S ribosomes were observed even in 5 mM Mg^{2+} , as in the wild-type strain [Figure 5b(1),(3)]. We also analyzed r-proteins from CRs by RFHR 2D-PAGE. The level of RMF, which is required for 100S formation, did not differ among the three strains [Figure 5a(1),(2),(3)]. In BW25113 $\Delta rpmE::Km zur$ (T200A), 100S formation was the same as in W3110 $\Delta rpmE::Km zur::IS2$ (Figure S5). These results indicated that ribosomes containing YkgM form 100S ribosomes to the same extent as ribosomes containing intact L31.

2.5 | In vitro translation activity of ribosomes containing YkgM

The in vitro translation activity of HSRs from W3110 $\Delta rpmE::Km$, which lack L31, was about 40% of that of HSRs from $\Delta ompT::Km$, which carry one copy of L31 (Figure 6a; Ueta et al., 2017). Hence, we investigated whether ribosomes of W3110 $\Delta rpmE::Km zur::IS2$, which contain one

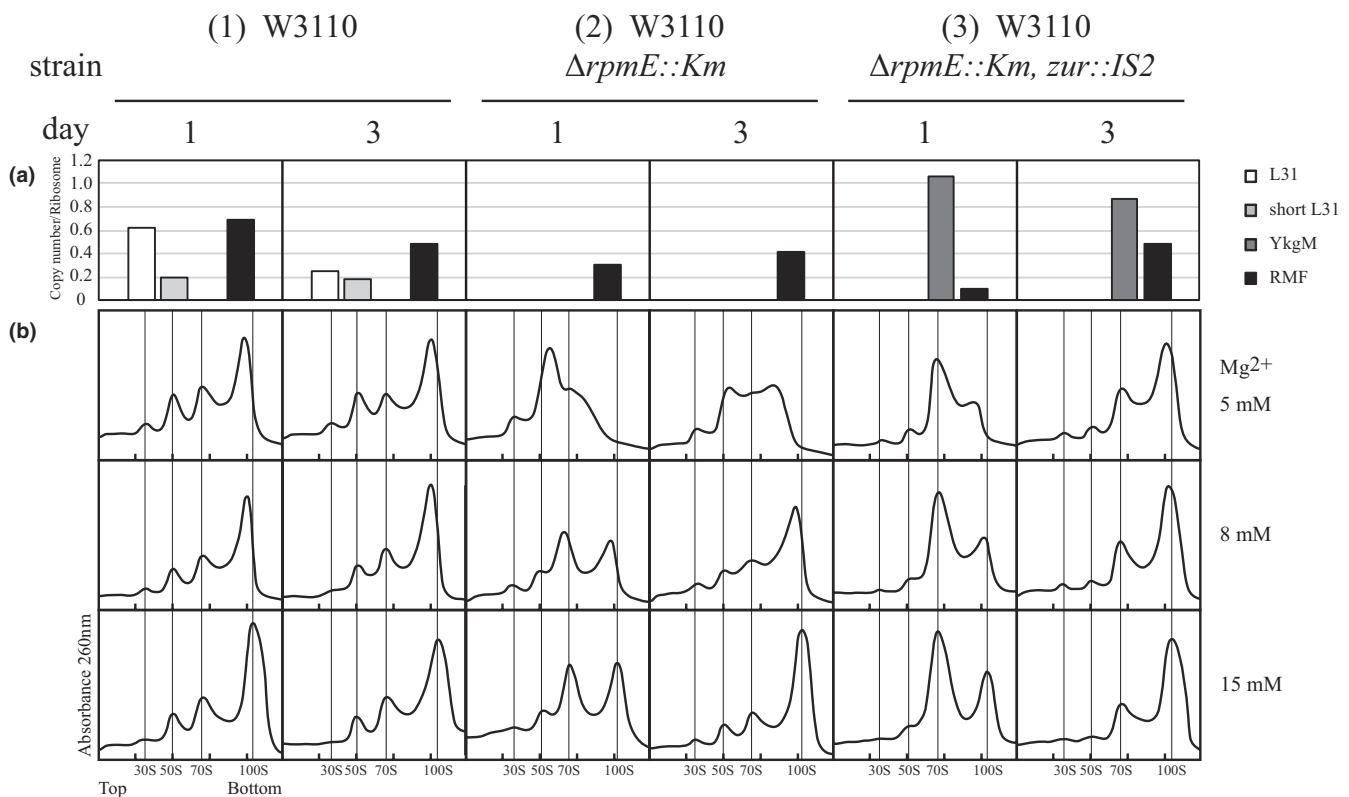


FIGURE 5 Ribosomes lacking L31 are defective in 100S formation in the stationary phase, but YkgM restores their function. (a) W3110 (1), $\Delta rpmE::Km$ (2) and $\Delta rpmE::Km zur::IS2$ (3) cells were grown at 37°C for 1 or 3 days in EP medium, and then harvested. Crude ribosomes (CRs) from each strain were prepared and analyzed by RFHR 2D-PAGE and 5%–20% SDG centrifugation with 5, 8 and 15 mM Mg^{2+} . Copy numbers per ribosome of intact L31 (white), short L31 (gray), YkgM (dark gray) and RMF (black) in each CR sample are shown in the bar graph. (b) Ribosome profiles after 5%–20% SDG centrifugation in 5, 8 and 15 mM Mg^{2+} are shown. For each CR sample, 150 pmol was used

copy of YkgM, recover translational activity. To this end, we measured synthesis of dihydrofolate reductase (DHFR) from the *folA* gene using a purified in vitro transcription–translation protein synthesis system (PUREflex 1.0 kit) (Ueta et al., 2017). In HSRs from $\Delta rpmE::Km$ *zur::IS2*, translational activity was the same as in HSRs from $\Delta ompT::Km$ (Figure 6a). These observations show that ribosomes containing YkgM have the same in vitro translational activity as those containing L31.

2.6 | Growth of $\Delta rpmJ$ is inhibited at 25, 37 and 42°C

To investigate the functions of L36, we examined growth at a range of temperatures. For these experiments, W3110 $\Delta ompT$, $\Delta ompT \Delta rpmJ$ and $\Delta ompT \Delta rpmJ \Delta zur::Km$ cells were cultured overnight at 37°C. The cultures were diluted 1:10⁶ in saline, spread 0.1 ml on L-broth plates and incubated for 1–4 days at 25, 37 or 42°C. Colony size was visualized by taking photographs of each plate every day for 4 days. The $\Delta ompT \Delta rpmJ$

strain formed smaller colonies than wild-type cells even after 4 days of incubation at all temperatures tested (Figure 7); in contrast to the wild type, colonies of the $\Delta ompT \Delta rpmJ$ strain were not clearly visible before 1 day of incubation at 37°C or 2 days of incubation at 25 or 42°C. Thus, growth of the $\Delta ompT \Delta rpmJ$ strain was especially strongly inhibited at nonoptimal temperatures. Colony size of the *zur* mutant, which expressed the L36 paralog YkgO, was the same as that of wild-type cells at all time points and temperatures (Figure 7). We examined whether the inhibition of growth causes by *rpmJ* gene. For this purpose, W3110 $\Delta rpmJ::Km/pBAD22$ and $\Delta rpmJ::Km/pBAD22-rpmJ^+$ cells were grown overnight at 37°C, diluted as described above, spread on L-broth plates containing 0.08% arabinose + 50 µg/ml ampicillin and incubated at 25, 37 or 42°C. Again, colony size was monitored by photographing the plates daily over 4 days. $\Delta rpmJ::Km/pBAD22-rpmJ^+$ cells formed normal colonies, whereas $\Delta rpmJ::Km/pBAD22$ did not (Figure S6(A)). Thus, growth inhibition was caused by deletion of *rpmJ* and rescued by expression of L36 from $pBAD22-rpmJ^+$. Furthermore, W3110 $\Delta ompT$, $\Delta ompT \Delta rpmJ$ *zur::Km* and $\Delta ompT \Delta rpmJ::Km$

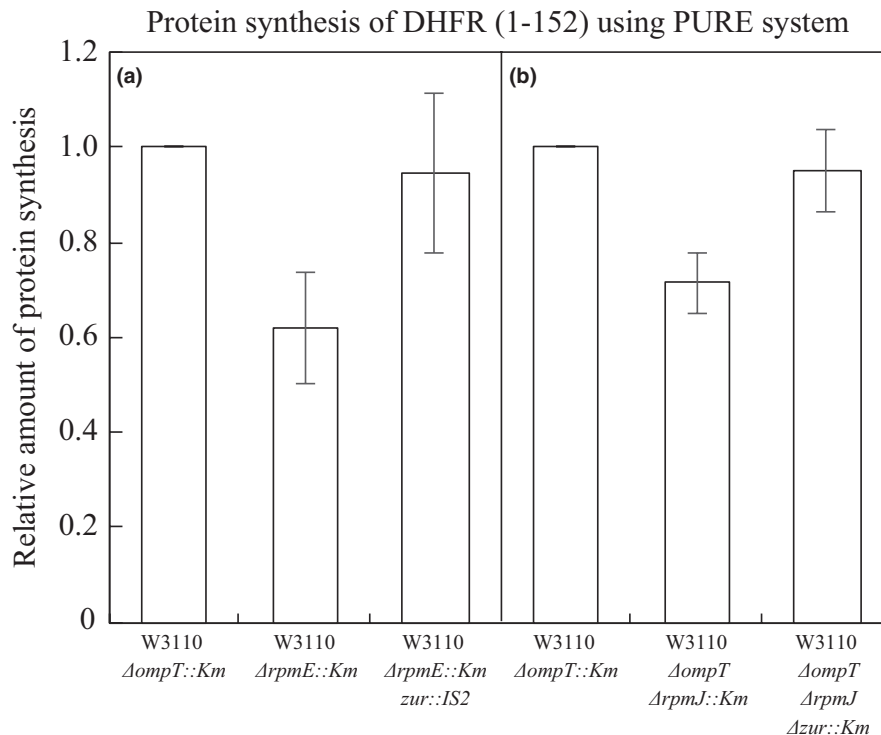


FIGURE 6 (a) In vitro translational activity of ribosomes lacking L31 is 40% lower than that of ribosomes containing intact L31, but ribosomes containing YkgM almost completely recover their function. Synthesis of DHFR (1–152) was measured using a purified in vitro transcription–translation system. High-salt-washed ribosomes (HSRs) prepared from three strains (W3110 $\Delta ompT::Km$, $\Delta rpmE::Km$ and $\Delta rpmE::Km$ *zur::IS2*) were added to the purified system. After electrophoresis of reaction mixtures on 10%–20% linear gradient SDS-PAGE gels, synthesized DHFR (1–152) was visualized by CBB. The density of the DHFR band was normalized against that of the r-protein band. Protein synthesis was normalized against synthesis by HSRs containing only intact L31 (i.e., $\Delta ompT::Km$). The data shown are averages of four independent reactions and two PAGE gels for each reaction (a total of eight gels). (b) Translational activity of ribosomes lacking L36 is 30% lower than that of ribosomes containing L36, but YkgO almost completely recover their function. Data were obtained as described in (a), except that the ribosomes were prepared by the method of Shimizu and Ueda (2010) from W3110 $\Delta ompT::Km$, $\Delta ompT \Delta rpmJ::Km$, $\Delta ompT$ and $\Delta rpmJ \Delta zur::Km$ cells

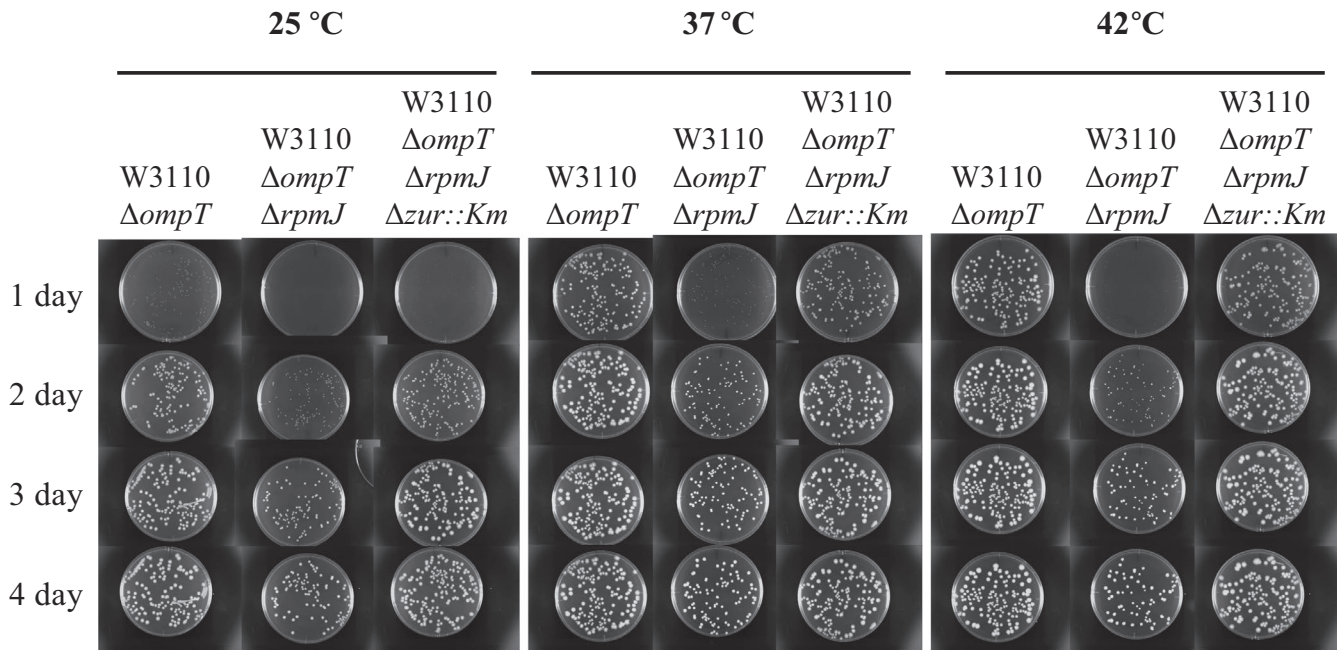


FIGURE 7 The *rpmJ* deletion mutant strain forms small colonies and grows more slowly than the wild type, but the $\Delta zur::Km$ mutation rescued the inhibition of growth at 25, 37 and 42°C. W3110 $\Delta ompT$, $\Delta ompT \Delta rpmJ$ and $\Delta ompT \Delta rpmJ \Delta zur::Km$ cells were grown overnight at 37°C. Each strain was diluted $1:10^6$ in saline and spread 0.1 ml on plates. The plates were incubated for 1–4 days at 25, 37 and 42°C. The colony size on each plate was measured in photographs

pBAD22-*rpmJ*⁺ cells were grown in EP liquid medium at 37°C and turbidity was measured every thirty minutes in the logarithmic growth phase and every day in the stationary growth phase. Doubling time of $\Delta ompT \Delta rpmJ::Km$ was 60 min but DT of wild type ($\Delta ompT$) was 45 min. $\Delta ompT \Delta rpmJ zur::Km$ and $\Delta ompT \Delta rpmJ::Km/pBAD22-rpmJ^+$ were DT = 45 min and 50 min, respectively (Figure S6B). In liquid culture, cells lacking L36 grow 33% later than wild-type cells ($\Delta ompT$) and the growth inhibition was recovered by *zur* mutant and pBAD22-*rpmJ*⁺. In the liquid EP medium, a result same as solid L medium culture was also observed.

2.7 | Association of 30S and 50S subunits and formation of 100S are not prevented by the lack of L36 or YkgO

W3110 $\Delta ompT::Km$, $\Delta rpmJ \Delta ompT::Km$ and $\Delta zur \Delta rpmJ \Delta ompT::Km$ cells were grown to 50 Klett units at 37°C, and HSRs were prepared from each strain. To examine subunit association in these HSRs, we performed SDG centrifugation under various Mg^{2+} concentrations (2, 3, 5, 6, 8, 10 and 15 mM). In contrast to our findings regarding L31, in ribosomes lacking L36, the association of 30S and 50S was not affected even in 5 mM Mg^{2+} , and the 70S ribosomes were observed as the main peak (compare Figure S7 with Figure 4a(2),(3)).

Ribosomes lacking L31 cannot form stable 100S ribosomes (Figure 5; Ueta et al., 2017). However, ribosomes

lacking L36 formed stable 100S in stationary phase (i.e., after culture for 1 or 3 days). In $\Delta rpmJ$ cells lacking L36 and YkgO, the level of 100S formation after 1 or 3 days of culture was essentially the same as in the wild type (Figure S8). W3110 $\Delta ompT::Km \Delta rpmJ \Delta zur$, which contains YkgM and YkgO but not L36, formed 100S ribosomes even after SDG centrifugation in 5 mM Mg^{2+} (Figure S8). Thus, ribosomes lacking L36 and its paralog YkgO are not deficient in 30S–50S association or 100S formation.

2.8 | Translation activity of L36 or YkgO in vitro

Next, we examined whether ribosomes lacking L36 have any influence on in vitro translation activity. Three strains, W3110 $\Delta ompT::Km$, $\Delta ompT \Delta rpmJ::Km$ and $\Delta ompT \Delta rpmJ \Delta zur::Km$, were cultured to 50 Klett units, and the cells were collected. Ribosomes were prepared from each strain as described in Section 4. In vitro transcription–translation activity of the ribosomes was determined using a purified system (the PUREflex 1.0 kit) (Shimizu, Kanamori, & Ueda, 2005; Shimizu & Ueda, 2010; Ueta et al., 2017). Ribosomes prepared from W3110 $\Delta ompT \Delta rpmJ::Km$, which did not contain L36 or its paralog YkgO, had ~30% less activity than ribosomes from W3110 $\Delta ompT::Km$ (wild type), which contained one copy of L36 (Figure 6b). Ribosomes prepared from $\Delta ompT \Delta rpmJ \Delta zur::Km$ cells, which contained one copy of YkgO (Figure 8b), recovered translation activity comparable

to ribosomes from W3110 $\Delta ompT::Km$ (Figure 6b). These observations show that L36 contributes to translation in vitro, as does its paralog YkgO, which restores normal translational activity to ribosomes lacking L36.

2.9 | *zur* mutant cells express *rpmE*, *ykgM*, *rpmJ* and *ykgO*, and contain ribosomes with a mixture of all four proteins

W3110 $\Delta ompT \Delta zur::Km$ mutant cells were grown in EP medium at 37°C and collected in logarithmic growth phase (Klett units: 50) or stationary growth phase (1 or 3 days of culture). HSRs (for logarithmic phase) or CRs (for stationary phase) were prepared, and r-proteins were analyzed by RFHR 2D-PAGE. In *zur*-defective mutant cells, *rpmE*, *ykgM*, *rpmJ* and *ykgO* were expressed, and L31 or YkgM and L36 or YkgO were incorporated into ribosomes. The sum of copy numbers of L31 and YkgM was ~1, and that of L36 and YkgO was 0.7–0.9 (Figure 8a), suggesting that each paralog pair shares a single binding site. The ribosomes contained YkgM than L31 (ratio: 21–59:1), but YkgO than L36 (1:2.5–3.8). These uneven proportions did not differ between logarithmic phase and stationary phase (1 or 3 days) (Figure 8a), suggesting that expression of these proteins and their insertion into ribosome are homeostatically regulated and non-phase-dependent.

Ribosomes of W3110 $\Delta ompT$ cells contained one copy of L31, and those of $\Delta rpmE zurIS2$ cells contained one copy of YkgM. If the expression levels of L31 and YkgM in $\Delta ompT \Delta zur::Km$ mutant cells are comparable to those in $\Delta ompT$ and $\Delta rpmE zur::Km$ cells, respectively, it means that YkgM binds to ribosomes in vivo with greater affinity than L31. Ribosomes of $\Delta ompT$ cells contain a single copy of L36. When *rpmJ* (L36) was deleted, ribosomes contained a single copy of YkgO (Figure 8b). If L36 and YkgO are present at comparable levels in W3110 $\Delta ompT \Delta zur::Km$ mutant cells, L36 is likely to have higher affinity for ribosomes than YkgO.

2.10 | $\Delta rpmJ$ is defective in late assembly of the 50S subunit

Chemical protection experiments suggested that L36 directly contacts four regions of the ribosome (helices 89 and 91 of 23S RNA, which stem from the peptidyl transferase center; bases in the stalk that binds L10/(L12)₄, and helix 97 in the four-helix junction containing the sarcin–ricin loop) and plays a significant role in organizing 23S rRNA structure (Maeder & Draper, 2005). Hence, we investigated whether the 50S subunit was assembled normally in cells lacking L36. The W3110 $\Delta rpmJ$ and wild-type strains were grown at 25, 37 and 42°C, and used to prepare CRs; these ribosome samples

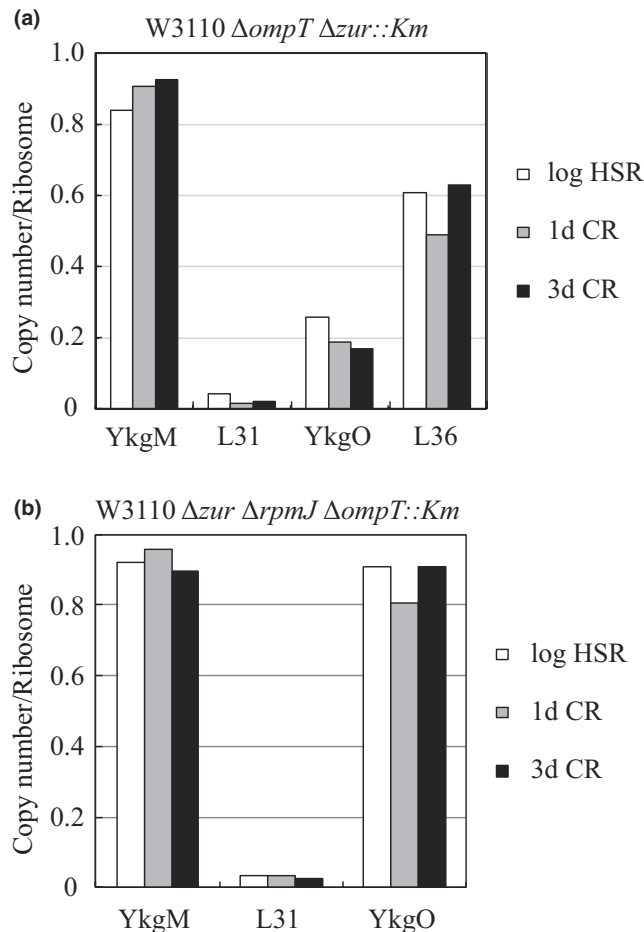


FIGURE 8 *zur* mutant cells express four genes (*rpmE*, *ykgM*, *rpmJ* and *ykgO*), and have four types of ribosomes containing L31 or its paralog YkgM and L36, or its paralog YkgO. (a) W3110 $\Delta ompT \Delta zur::Km$ and (b) $\Delta zur \Delta rpmJ \Delta ompT::Km$ mutant cells were grown in EP medium at 37°C and collected in logarithmic growth phase (Klett unit: 50) or stationary phase (1 and 3 days). HSRs (for the logarithmic phase) or CRs (for stationary phase) were prepared, and the r-proteins were analyzed by RFHR 2D-PAGE. In *Zur*-defective mutant cells, four genes (*rpmE*, *ykgM*, *rpmJ* and *ykgO*) were expressed, and L31 or its paralog YkgM, and L36 or its paralog YkgO were incorporated into ribosomes. The copy numbers of L31, YkgM, L36 or YkgO in the HSR or CR were analyzed by RFHR 2D-PAGE. The vertical axis shows copy number per ribosome. Copy numbers of L31, YkgM, L36 or YkgO in ribosomes prepared from logarithmic phase (Klett unit: 50) (white) or cells cultured for 1 day (gray) or 3 days (black) are shown

were analyzed by SDG centrifugation at 15 or 0.5 mM Mg²⁺. In sedimentation profile of the ribosomes of wild-type CRs at 25, 37 and 42°C, 30S and 50S subunits were predominant in 0.5 mM Mg²⁺, whereas 70S ribosomes were predominant in 15 mM Mg²⁺. Analysis of r-proteins by RFHR 2D-PAGE yielded normal constitutive profiles (Figure S9). On the other hand, in CRs from $\Delta rpmJ$ cells, an unexpected smaller peak at 40S was observed in 0.5 mM Mg²⁺ (Figure 9a). The 40S

and 50S fractions of $\Delta rpmJ$ cells were collected, and the r-proteins were analyzed by RFHR 2D-PAGE. The 50S r-proteins from the $\Delta rpmJ$ cells had the same profile as those from wild-type 50S, whereas r-proteins from the 40S fraction lacked L16 and L35, which are late assembly proteins (Figure 9b; Figure S9). This observation shows that the 40S subunit is an intermediate of 50S subunit assembly into which L16 and L35 have not yet been incorporated, suggesting that $\Delta rpmJ$ cells take longer than wild-type cells for late-stage assembly of the 50S subunit.

3 | DISCUSSION

We first discovered L36, along with L35, by RFHR 2D-PAGE, which is well suited to the detection of small basic proteins (Wada, 1986a, 1986b; Wada & Sako, 1987). L36 is the smallest and most highly basic r-protein, with a theoretical pI of 10.69 and MW of 4,364.33. Consequently, it could not have been detected by the traditional 2D-PAGE method (Kaltschmidt & Wittmann, 1970). L36 is widely conserved in bacteria, chloroplasts and mitochondria, but not in archaea or the nuclear genome of eukaryotes. Furthermore, intact L31 (70 amino acids), but not the short form (62 amino acids), which was misidentified as the full-length protein by Kaltschmidt & Wittmann, was also detected by RFHR 2D-PAGE (Wada, 1998; Wada et al., 1990).

Ribosomes lacking L31 were 40% less active than wild-type ribosomes in an in vitro transcription–translation system (Figure 6a; Ueta et al., 2017). In these ribosomes, peptide elongation is slower, 30S and 50S subunit association in vivo and in vitro is weakened, and 100S ribosomes are not formed in the stationary phase (Figure 4a,b; Figure 5; Ueta et al., 2017). L31 was defined as a 50S r-protein (Kaltschmidt & Wittmann., 1970), but it has an extremely specific binding mode which bridges 50S with the N-terminal half and 30S with the C-terminal half, and interacts with L5, S13, S19 and S14. Therefore, ribosomes lacking L31 may give rise to negative structural changes to not only 50S but also 30S, and fails to translational function, subunit association and 100S formation. On the other hand, ribosomes lacking L36 were 30% less active than wild-type ribosomes in vitro but correctly formed 70S from 30S and 50S subunits both in

vivo and in vitro (Figure 6b; Figure S7), and like wild-type ribosomes could also form 100S ribosomes during stationary phase (Figure S8). Therefore, L36 probably does not contribute to 70S association and 100S formation.

Zinc-binding proteins in ribosomes are widely conserved among bacteria. In many gamma-proteobacteria, including *Escherichia coli*, both L31 and L36, and their paralogs are conserved; notably, however, the paralogs have no zinc-binding sites (Table S3).

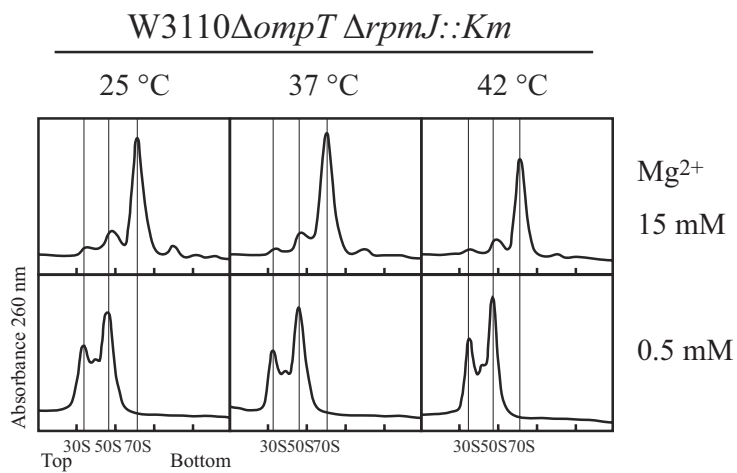
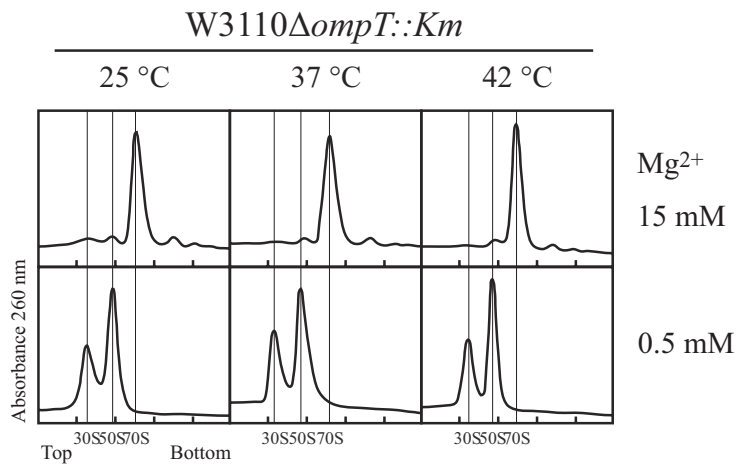
In this study, to understand the functional relationships of these two pairs of paralogs in regard to some functions containing translational activity and Zur regulation, we constructed five strains: *zur* mutant, single deletions of *rpmE* and *rpmJ*, and double-deletion mutants of *zur* & *rpmE* and *zur* & *rpmJ*. Ribosomes from the *zur rpmE* mutant, which contained one copy of YkgM, were functionally equivalent to wild-type ribosomes (which contain one copy of L31) in terms of the association of 30S and 50S subunits (Figure 4a,b; Figure S4A,B), in vitro translational activity (Figure 6a), 100S formation (Figure 5) and cell growth (Figure 1a–c; Figure S2A–C), indicating that YkgM is functionally identical to L31 in these contexts.

Ribosomes containing one copy of YkgO were also functionally equivalent to wild-type ribosomes (which contain one copy of L36) in in vitro translational activity (Figure 6b) and cell growth (Figure 7; Figure S6B). It suggests that zinc atom bound to L31 or L36 is not involved in these processes. On the other hand, it is known that L31 and L36 are related to Zn storage and provision in vivo. Under conditions of zinc starvation, non-Zn-ribbons paralogs are expressed, leading to incorporation of the paralogs into ribosomes in place of the original Zn-binding r-proteins, and thus, released zinc atoms are used by other cellular zinc-binding proteins such as DNA polymerase and primase (Gabriel & Helmann., 2009; Nanamiya et al., 2004; Owen, Pascoe, Kallifidas, & Paget, 2007; Panina et al., 2003; Shin & Helmann., 2016). Our results also suggest that L31 and L36 may be related to Zn storage and provision in vivo.

All four mutation sites in spontaneous mutants isolated from $\Delta rpmE$ were located in the *zur* gene (Figure 2). Two of the mutants involved insertion mutations of IS into *zur*, and the other two were caused by point mutations. The Zur monomer includes two domains, an N-terminal

FIGURE 9 In the *rpmJ* deletion mutant strain, 40S particles were observed after SDG centrifugation in 0.5 mM Mg²⁺. (a) W3110 $\Delta ompT::Km$ (wild type) and $\Delta ompT \Delta rpmJ::Km$ cells were grown at 25, 37 and 42°C. Crude ribosomes were prepared from each strain and analyzed by SDG centrifugation in 15 or 0.5 mM Mg²⁺. The ribosome profiles are shown in the top (W3110 $\Delta ompT::Km$) and bottom (W3110 $\Delta ompT \Delta rpmJ::Km$) panels. (b) The r-proteins in the 40S fraction did not contain L16 and L35, in contrast to those in the 50S fraction. The upper panel in b(1) shows the ribosome profile after SDG centrifugation (10%–40% sucrose, 31,500 g, 44 hr, SW41Ti) in 0.5 mM Mg²⁺. 40S or 50S fractions were collected, and each collected fraction was confirmed by SDG centrifugation (left panel: same as upper panel; right panel: 10%–40% sucrose, 35,600 g, 19.5 hr, SW41Ti) in 0.5 mM Mg²⁺ [b(1) bottom panel]. R-proteins of the collected 40S or 50S fractions were analyzed by RFHR 2D-PAGE. Copy numbers of L16 and L35 differed significantly between the 40S and 50S fractions. Copy numbers are shown in b(2). White and gray squares show copy numbers of L16 and L35 in the 50S and 40S fractions, respectively. Black squares show copy numbers in 40S particle, which corrected L16 and L35 in 50S fractions carried to 40S fractions

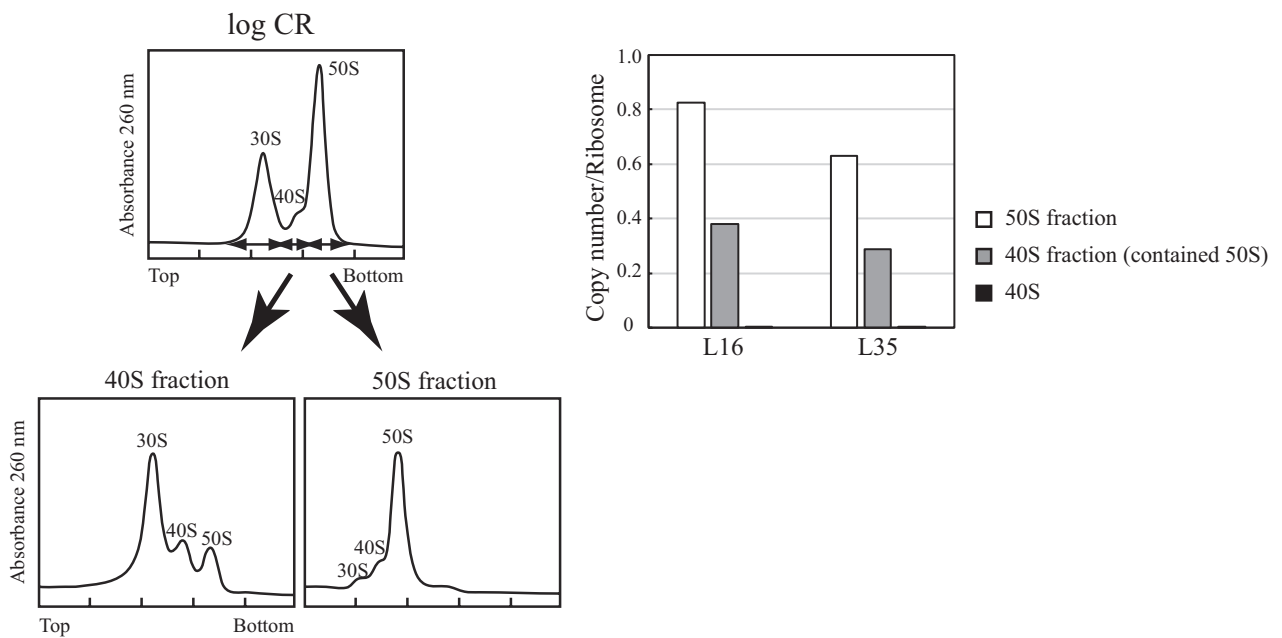
(a)



(b)

(1) *W3110 $\Delta ompT \Delta rpmJ::Km$*

(2)



DNA-binding domain ($\alpha 2$ – $\alpha 4$, amino acids 23–72) and a C-terminal dimerization domain ($\alpha 5/\beta 5$, amino acids 115–141). A dimer of Zur dimers, (Zur₂)₂, interacts specifically with promoter DNA (33-mer) in the *zur* regulon and is essential for promoter region binding (Gilston et al., 2014). One of the point mutations, T200A/Leu67Gln, altered a residue in the DNA-binding region of Zur. The other point mutant was G422A/Gly141Glu, located in the dimerization domain. It is likely that neither of the mutant Zur proteins can bind to the promoter of the *ykgM*–*ykgO* operon. The IS insertions occurred 25 and 59 nucleotides from the 5' end of the *zur* gene, and insertion into the N-terminus probably interferes with promoter binding. It is likely that all four *zur* mutants are unable to bind the *ykgM*–*ykgO* promoter, resulting in constitutive induction of *ykgM* and *ykgO*. The frequency of *zur* mutation in the $\Delta rpmE$ strain was not particularly high, comparable to the frequency of Nal-resistance mutations.

The *rpmJ* gene is not essential for growth at 37°C in L-broth (Baba et al., 2006), but cells lacking this gene grew more slowly than wild-type or *ykgO*-expressing cells (Figure 7; Figure S6A,B). This tendency was particularly evident at lower (25°C) or higher temperature (42°C) (Figure 7). Ikegami, Nishiyama, Matsuyama, and Tokuda (2005) reported that an insertion mutant of *rpmJ* might affect the expression of *secY*, which precedes *rpmJ* in the *spc* operon, resulting in slow growth. However, the growth inhibition observed in the *rpmJ* mutant we used was suppressed by providing L36 on a plasmid harboring *rpmJ*⁺ (Figure S6A,B), but not complemented by a plasmid harboring *secY*: wild-type DT, 20 min; $\Delta rpmJ$ strain DT, 45 min; $\Delta rpmJ$ /Aska *secY*⁺ strain DT, 45 min. This indicates that L36 or its paralog YkgO is involved in growth. The growth defect in the *rpmJ* mutant had been previously reported (Maeder & Draper, 2005).

Chemical protection experiments identified four regions in the 50S subunit as possible direct contact sites between 23S RNA and L36: helices 89 and 91, which stem from the peptidyl transferase center; helix 42, the rRNA stem that binds L10/(L12)₄; and helix 95 in the four-helix junction containing the sarcin–ricin loop. The tertiary interactions between helices 89, 91 and 95 are disrupted in ribosomes lacking L36, supporting the argument that L36 plays a significant role in organizing 23S rRNA structure (Maeder & Draper, 2005). Helix 89 of 23S rRNA is very important for the functional regions of the ribosome, including the peptidyl transferase center and elongation factor binding site. Consistent with this, the secondary structure of helix 89, determined by X-ray structural analysis, showed that the tertiary contacts of helices 89, 91 and 95 are also important for ribosome function (Burakovsky et al., 2011). This suggests that in our ribosomes lacking L36, the reduction of in vitro translation activity was caused by a structural change in the peptidyl transferase center of 23S RNA.

50S subunit biogenesis is performed by RNA helicases (DeaD, DbpA, SrmB, RhlE), RNA modification enzymes [RlmE (FtsJ, RrmJ, MrsF), RluB (YciL), RluC, RluD], chaperones (DnaK/DnaJ/GrpE, GroES/GroEL) and GTPases [ObgE (CgtAE), Der, YihA, BipA, RbgA] (Britton, 2009; Hager, Staker, Bugl, & Jakob, 2002; Iost, Bizebard, & Dreyfus, 2013; Kaczanowska & Rydén-Aulin, 2007; Leppik, Liiv, & Remme, 2017; Shajani, Sykes, & Williamson, 2011). When these functions are defective, pre-50S subunits (40S or 45S) are observed along with 30S and 50S in SDG centrifugation at low Mg²⁺ (Shajani et al., 2011). The 40S and 45S intermediate particles lack some ribosomal proteins; for example, in the 40S particle formed in the $\Delta srmB$ strain, the levels of L6, L7/L12, L14, L16, L25, L27, L31, L32 and L33 are reduced, and L13, L28 and L34 are missing (Charollais, Pflieger, Vinh, Dreyfus, & Lost, 2003). In the 40S particle formed by the *csdA* mutant, L6, L16, L25, L28, L32, L33 and L34 are present at dramatically reduced levels (Charollais, Dreyfus, & Lost, 2004). In the 45S particle from a mutant in the RNA helicase *dbpA*, the levels of L16, L25, L27, L28, L33, L34 and L35 were significantly reduced (Elles, Sykes, Williamson, & Uhlenbeck, 2009). In the 45S particle of the $\Delta rlmE$ mutant, the levels of L5, L6, L16, L18, L19, L25 and L27 are reduced, and L35 is significantly less abundant (Arai et al., 2015). Quantitative mass spectrometry has shown that the r-proteins L7/L12, L10, L16, L25, L27, L30, L35 and L36 belong to the late (or “fifth”) assembly group (Chen & Williamson, 2013). In our results, the 40S intermediate particle in *rpmJ* cells lacked L16 and L35, which are late assembly r-proteins, whereas the other r-proteins in the 50S particle did not differ between wild-type and $\Delta rpmJ$ strains. Furthermore, 50S or 70S particles from *rpmJ* cells contained the same r-proteins as those from wild-type cells. Together, these findings imply that the 40S is an intermediate of the 50S subunit. Deficiency of L36 causes a structural change in 23SRNA, preventing late assembly from advancing normally and causing accumulation of a 40S intermediate particle that lacks L16 and L35. This suggests that L36 is involved in incorporation of L16 and L35 into the ribosome in the final step of late assembly. Whether L36 itself participates directly or indirectly in ribosome assembly is a matter that should be addressed in future studies.

When *E. coli* is cultured in the mops medium at 37°C, YkgM is expressed in the stationary phase from late log phase (Lilleorg et al., 2019). However, when we carried out experiments using wild-type strains (W3110 and W3110 $\Delta ompT$) cultured in EP medium at 37°C, the stationary phase-specific protein RMF was expressed, but YkgM was expressed in neither logarithmic phase (Figure 3) nor stationary phase (Figure 6), as in the W3110 $\Delta ykgM$ strain. Expression of *ykgM* and *ykgO* is regulated by the Zur repressor. When Zur is inactivated by zinc depletion (Gilston et al., 2014) or the *zur* gene is mutated, *ykgM* and *ykgO* are expressed from the *ykgM*–*ykgO* operon. Under our culture conditions, the zinc concentration during stationary phase was sufficient for Zur

repression. Therefore, Zur repression may depend solely on zinc concentration even in stationary phase. It is possible that YkgM and YkgO were expressed due to zinc depletion rather than induction by stationary phase.

In wild-type cells, one copy each of L31 and L36 binds to 50S subunits in all growth phases. In *zur* deletion mutants of *rpmE* (L31) or *rpmJ* (L36), one copy each of YkgM or YkgO, respectively, binds to 50S subunits (Figure 8b). On the other hand, in *zur* mutant cells, L31, L36, YkgM and YkgO were observed simultaneously in ribosomes (Figure 8a). We measured the copy numbers of these four proteins by RFHR 2D-PAGE. The sum of copy numbers of L31 and YkgM was one, indicating that the two proteins share a single binding site on the 50S subunit. Similarly, the sum of copy numbers of L36 and YkgO was also approximately one, likewise suggesting a single binding site (Figure 8a). Recently, it was established by X-ray structure of 70S ribosome that L31 & YkgM, and L36 & YkgO share identical ribosome-binding sites to L31 and L36 (Lilleorg et al., 2019).

4 | EXPERIMENTAL PROCEDURES

4.1 | Bacterial strains and plasmids

All strains used in this study are shown in Table S1. W3110 $\Delta ykgM::Km$ (YB1011) and W3110 $\Delta rpmJ::Km$ (YB1026) were constructed by P1vir transduction of the recipient strain W3110 (wild type). Deletion mutants of *ykgM* and *rpmJ* (BW25113-derived strains; JW5035-1, JW3261-1) were obtained from the *E. coli* Keio Knockout Collection (Baba et al., 2006), and P1vir phages from the two strains were prepared and used as donors. In each strain constructed, exchange of the kanamycin-resistance gene *Km* for the *ykgM* and *rpmJ* genes was confirmed by PCR. W3110 $\Delta rpmE$, $\Delta ompT$, $\Delta rpmJ$ and Δzur mutants were constructed by elimination of the kanamycin-resistance cassette from W3110 $\Delta rpmE::Km$, $\Delta ompT::Km$, $\Delta rpmJ::Km$ and $\Delta zur::Km$, respectively, using a helper plasmid (pCP20) encoding the FLP recombinase (Datsenko & Wanner, 2000). The double-deletion mutants W3110 $\Delta rpmE \Delta ykgM::Km$ (YB1013), $\Delta zur \Delta rpmJ::Km$ (YB1027), $\Delta rpmJ \Delta ompT::Km$ (YB1028), $\Delta ompT \Delta rpmJ::Km$ (YB1029) and $\Delta ompT \Delta zur::Km$ (YB1031) were constructed using donor P1vir phage from BW25113 $\Delta ykgM::Km$, $\Delta rpmJ::Km$, $\Delta ompT::Km$ and $\Delta zur::Km$ via general transduction of recipient strains W3110 $\Delta rpmE$, $\Delta ompT$, $\Delta rpmJ$ and Δzur , respectively. All double-deletion strains were confirmed by PCR. The four spontaneous *zur* mutants W3110 $\Delta rpmE::Km zur::IS2$ (YB1018), $\Delta rpmE::Km zur::IS1$ (YB1024), $\Delta rpmE::Km zur::G422A$ (YB1025) and BW25113 $\Delta rpmE::Km zur::T200A$ (YB1022) were isolated by large-colony selection from YB1010

(W3110 $\Delta rpmE::Km$) or JW3907-1 (BW25113 $\Delta rpmE::Km$), which grew slowly and formed small colonies. The mutation sites in the *zur* gene were determined by DNA sequencing (Figure 2).

Plasmids used were as follows: ASKA clones (Kitagawa et al., 2005), JW3262 (pCA24N-*secY*⁺ without GFP), JW3261 (pCA24N-*rpmJ*⁺ without GFP) and pBAD22-*rpmJ*⁺. The multiple cloning site of pBAD22 (Guzman, Belin, Carson, & Beckwith, 1995) was cleaved with *EcoRI* and *HindIII*, and replaced with the *EcoRI-rpmJ-HindIII* fragment, which was constructed by amplifying chromosomal DNA from W3110 wild-type cells with primers 5'-GCCATGAATTCAAAGTTCGTGCTTC-3' and 5'-ACAGCGCCAAGGCTGAAAGCTTGCC-3'; the amplicon was digested with *EcoRI* and *HindIII*.

4.2 | Media and growth conditions

All strains were grown in medium E supplemented with 2% polypeptone and 0.5% glucose (EP medium) (Wada, 1986a), at 37°C. Cell growth was monitored by measuring turbidity using a Klett Summerson photoelectric colorimeter (Bel-Art Product, Wayne, NJ, USA) with a green filter (#54). Cells were harvested in exponential and/or stationary phases, and stored at -80°C until use. Cell growth on L-broth agar plates was determined by colony size after 1–4 days of incubation at 25, 37 or 42°C.

4.3 | Determination of mutation sites in the four spontaneous suppressor mutants of $\Delta rpmE$

The four mutants were grown at 37°C, and each genomic DNA was prepared using the Gentra Puregene Yeast/Bacteria Kit (QIAGEN). PCR was performed on chromosomal DNA using PCR primers for the *zur* gene and promoter region of *ykgM* (Table S2) and GoTaq Green Master Mix (Promega). The four PCR products were purified by QIAquick PCR purification kit (QIAGEN), and the sequencing of purified PCR products was performed by Fasmac (Ltd.). The primers used were *zur* (up) and *zur* (down) for YB1024, YB1025 and YB1022, and *zur* (up) and *insAB* (down), and *insA* (up) and *zur* (down) for YB1018 (Table S2).

4.4 | Ribosome preparations and analyses

4.4.1 | Preparations of CRs

CRs were prepared from cell extracts according to the method of Noll, Hapke, Schreire, and Noll (1973) with slight modifications

(Horie, Wada, & Fukutome, 1981). Cells harvested at the indicated times were ground with similar volumes of quartz sand (Wako) and then extracted with buffer I [20 mM Tris-HCl (pH 7.6), 15 mM magnesium acetate, 100 mM ammonium acetate and 6 mM 2-mercaptoethanol]. The homogenate was centrifuged at 9,000 *g* for 15 min at 4°C. The supernatant was saved, and the pellet was re-suspended in buffer I. The suspension was centrifuged again under the same conditions. The pellet was termed the cell debris (CD) fraction. The combined supernatants (cellular extracts, CEs) were layered onto a 30% sucrose cushion in buffer I and centrifuged in a 55.2 Ti rotor (Beckman) at 206,000 *g* for 3 hr at 4°C. The pellet was re-suspended in buffer I. This suspension was used as CRs.

4.4.2 | Preparation of high-salt-washed ribosomes (HSRs)

HSRs were prepared as described by Horie et al. (1981). CRs were re-suspended in buffer II [20 mM Tris-HCl (pH 7.6), 10 mM magnesium acetate, 1 M ammonium acetate and 6 mM 2-mercaptoethanol]. After mixing for 1 hr at 4°C, the high-salt-washed suspension (20 ml) was layered onto a 30% sucrose cushion in buffer II (10 ml) and centrifuged in a 55.2 Ti rotor (Beckman) at 206,000 × *g* for 4 hr at 4°C. The pellet was re-suspended in buffer I and dialyzed against buffer I overnight. This suspension was used as HSRs.

4.4.3 | Preparation of 30S and 50S subunits

High-salt-washed ribosomes were suspended in dissociation buffer I [20 mM Tris-HCl (pH 7.6), 1 mM magnesium acetate, 100 mM ammonium acetate and 6 mM 2-mercaptoethanol] and dialyzed against the same buffer overnight. The sample was layered onto a 10%–40% SDG in dissociation buffer I and centrifuged in a 45 Ti rotor (Beckman) at 20,000 *g* for 19 hr at 4°C. The gradient was fractionated, and the absorbance of each fraction was measured with a UV-1800 spectrometer (Shimadzu) at 260 nm. The 30S and 50S fractions were collected, and each subunit was pelleted by centrifugation in a 55.2 Ti rotor (Beckman) at 206,000 *g* for 4 hr at 4°C. Each pellet was re-suspended in buffer I.

4.4.4 | Analysis of ribosomes by SDG centrifugation

Each ribosome sample was layered onto a 5%–20% SDG in buffer I or modified Mg²⁺ buffer I [20 mM Tris-HCl (pH 7.6), 2–15 mM magnesium acetate, 100 mM ammonium acetate and 6 mM 2-mercaptoethanol] and centrifuged in an SW 40 Ti rotor (Beckman) at 25,000 *g* for 20 hr at 4°C. The

SDGs were prepared using Gradient maker (GRADIENT MATE 6T; BioComp Instruments). The absorbance of each fraction was measured at 260 nm using a flow cell in a UV-1800 spectrometer (Shimadzu).

4.5 | RFHR 2D-PAGE

E. coli r-proteins were prepared by the acetic acid method (Hardy, Kurland, Voynow, & Mora, 1969). One-tenth volume of 1 M MgCl₂ and two volumes of acetic acid were added to the ribosomal solutions, and the mixture was stirred for 1 hr at 0°C. After centrifugation at 10,000 *g* for 10 min, the supernatant was dialyzed three times against 2% acetic acid (the volume of the dialysis buffer was 300-fold larger than the volume of the sample) for 24 hr. The proteins were lyophilized and stored at –80°C until use. The protein solution (2 mg protein in 100 μl of 8 M urea containing 0.2 M 2-mercaptoethanol) was analyzed by RFHR 2D-PAGE as described previously (Wada, 1986a,b), with some slight modifications (Ueta, Wada, & Wada, 2010). The RFHR 2D-PAGE (radical-free and highly reducing two-dimensional-polyacrylamide gel electrophoresis) was produced by improving the Kaltschmidt and Wittmann's 2D-PAGE (Kaltschmidt & Wittmann, 1970) in the following points. (a) Gelation of sample solution was not performed to avoid immobilization of proteins by free radical fixation to the sample gels. Instead, for preparing sample gels, before the first dimension (1D) electrophoresis, another “sample charging electrophoresis” was performed to charge proteins into gel pieces polymerized previously in the reduced conditions. (b) In every electrophoresis, proteins migrated together with charged reductants, 2-aminoethanethiol to avoid formation of artificial disulfide bridges during migration. (c) The second dimension (2D) electrophoresis was carried out at a more acidic pH, 3.6, to get better separation of very small and basic proteins. With these modifications, quantitative yield and reproducibility became much better, and many faint spots disappeared not only at the high molecular weight side but also in the region containing primary spots of ribosomal proteins. Sample charging electrophoresis was carried out at 100 constant volts (CV) for 15 min at room temperature (RT). Subsequently, one-dimensional electrophoresis was carried out at 170 CV for 8 hr at RT, and two-dimensional (2D) electrophoresis was carried out at 100 CV for 15 hr at RT. The 2D gels were stained with CBB G-250, and protein spots were scanned using a GS-800 calibrated densitometer (Bio-Rad Laboratories).

4.6 | Determination of the ribosomal protein copy number

“Copy number” refers to the molar ratio of a ribosome-binding protein to a single 70S ribosomal particle, 30S subunit or

50S subunit. The OD of a protein spot on a RFHR 2D-PAGE gel was determined by scanning the spot with a GS-800 calibrated densitometer. The molar amount of the protein was proportional to its OD value (OD/MW). The OD/MW was calculated as a function of molecular weight, and the values for the intact L31, short L31 and RMF proteins were normalized against the OD/MW value for the r-proteins L27, L29 and L30. The r-proteins used for normalization were L21, L23 and L25 for YkgM, and L32, L33 and L35 for L36 and YkgO. These r-proteins were used as protein copy number markers because their copy numbers are known (Hardy, 1975; Tal, Weissman, & Silberstein, 1990; Wada, 1986a) and are near the spots corresponding to intact L31, short L31, RMF, YkgM, L36 and YkgO.

4.7 | In vitro dissociation and re-association of the 30S and 50S subunits

High-salt-washed ribosomes were prepared from CRs of mid-exponential cells and dialyzed against dissociation buffer II [20 mM Tris-HCl (pH 7.6), 1 mM magnesium acetate, 30 mM ammonium acetate and 6 mM 2-mercaptoethanol] overnight to dissociate the 30S and 50S subunits. To confirm the dissociation of the ribosomal subunits, the solutions were subjected to a 5%–20% SDG in dissociation buffer I and centrifuged in a SW 40 Ti rotor (Beckman) at 200,200 g for 2.5 hr at 4°C. The dissociated ribosomal subunits were exchanged into buffer I and incubated at 37°C for 30 min to re-associate the subunits into the 70S complex. The mixtures were analyzed by 5%–20% SDG centrifugation in the presence of either 15 or 6 mM Mg²⁺.

4.8 | In vitro translation assay

In vitro transcription–translation protein synthesis (Shimizu et al., 2005) was performed using the PUREflex 1.0 kit (GeneFrontier). The ribosomes in kit component Solution III were replaced with the high-salt-washed ribosomes prepared from W3110 $\Delta ompT::Km$, $\Delta rpmE::Km$ and $\Delta rpmE::Km zur::IS2$ (for Figure 6a) as described in our previous study (Ueta et al., 2017). For Figure 6b, the ribosomes of W3110 $\Delta ompT::Km$, $\Delta ompT \Delta rpmJ::Km$ and $\Delta ompT \Delta rpmJ \Delta zur::Km$ were prepared from the mid-exponential cells using HiTrap Butyl FF column (GE Healthcare Life Sciences) (Shimizu et al., 2005; Shimizu & Ueda, 2010). To clearly separate the in vitro synthesized protein from other proteins by the analysis of SDS-PAGE, DNA encoding DHFR (1–152 a.a.) was amplified from cDNA of DHFR (1–159 a.a.) using PCR primers 5'-GAAATTAATACGACTCACTATAGGGGAGACC-3' and 5'-GATAGCTCAGCTAATTAGCAATAGCTGTGA GAGTT-3'. The amplicon was purified by QIAquick PCR

purification kit (QIAGEN) and used as the template DNA in the transcription–translation reaction. The reactions were carried out for 2 hr at 37°C in a 20 μ l reaction mixture, containing 1 μ M ribosomes, 20 ng template DNA and 10 units RNase Inhibitor (Super) (Wako). The reaction mixtures were analyzed by SDS-PAGE using Multi Gel II mini 10%–20% linear gradient gel (Cosmo Bio Inc.). After CBB staining, gel bands were scanned using a GS-800 calibrated densitometer (Bio-Rad Laboratories) to measure the density of the synthesized protein.

4.9 | Preparation of 40S fraction

W3110 $\Delta ompT \Delta rpmJ::Km$ cells were grown at 37°C in EP medium and collected in logarithmic growth phase (Klett units: 50). CRs were prepared and dialyzed against dissociation buffer II overnight. The sample was layered onto a 10%–40% SDG in dissociation buffer III [20 mM Tris-HCl (pH 7.6), 0.5 mM magnesium acetate, 100 mM ammonium acetate and 6 mM 2-mercaptoethanol] and centrifuged in a 70 Ti rotor (Beckman) at 40,000 g for 21 hr at 4°C. The gradient was fractionated, and the absorbance of each fraction was measured with a UV-1800 spectrometer (Shimadzu) at 260 nm. The respective 40S or 50S fractions were collected. Each collected fraction was concentrated. Sucrose was removed, and the buffer was replaced with dissociation buffer I using an Amicon Ultra filter (100K; Millipore). For sedimentation profile of the ribosome, the CR, 40S or 50S fractions were layered onto 10%–40% SDG in dissociation buffer III and centrifuged in an SW 41 Ti rotor (Beckman) at 31,500 g for 44 hr at 4°C. The absorbance of each fraction at 260 nm was measured using a flow cell within a UV-1800 spectrometer (Shimadzu). The proteins of 40S and 50S fractions were analyzed by RFHR 2D-PAGE. The copy number of L16 was normalized against the values for the area containing L13, L14, L15, L17 and L18. The copy numbers of L35 were normalized against the values for L32 and L33. These r-proteins were used as protein copy number markers because their copy numbers are known (Hardy, 1975; Tal et al., 1990; Wada, 1986a), and they are near the spots corresponding to L16 and L35 proteins, respectively.

ACKNOWLEDGMENTS

The KEIO collection (Baba et al., 2006) and ASUKA clone strains (Kitagawa et al., 2005) were obtained from H. Mori at NAIST.

ORCID

Masami Ueta  <https://orcid.org/0000-0002-2858-0946>

Chieko Wada  <https://orcid.org/0000-0003-2924-3594>

Akira Wada  <https://orcid.org/0000-0002-8810-8264>

REFERENCES

- Agirrezabala, X., Liao, H. Y., Schreiner, E., Fu, J., Ortiz-Meoz, R. F., Schulten, K., ... Frank, J. (2012). Structural characterization of mRNA-tRNA translocation intermediates. *Proceedings of the National Academy of Sciences of the United States of America*, *109*, 6094–6099. <https://doi.org/10.1073/pnas.1201288109>
- Arai, T., Ishiguro, K., Kimura, S., Sakaguchi, Y., Suzuki, T., & Suzuki, T. (2015). Single methylation of 23S rRNA triggers late steps of 50S ribosomal subunit assembly. *Proceedings of the National Academy of Sciences of the United States of America*, *112*(34), E4707–E4716. <https://doi.org/10.1073/pnas.1506749112>
- Baba, T., Ara, T., Hasegawa, M., Takai, Y., Okumura, Y., Baba, M., ... Mori, H. (2006). Construction of *Escherichia coli* K-12 in-frame, single-gene knock-out mutants the Keio collection. *Molecular Systems Biology*, *2*, 2006.0008. <https://doi.org/10.1038/msb4100050>
- Britton, R. A. (2009). Role of GTPase in bacterial ribosome assembly. *Annual Review of Microbiology*, *63*, 155–176. <https://doi.org/10.1146/annurev.micro.091208.073225>
- Brosius, J. (1978). Primary structure of *Escherichia coli* ribosomal protein L31. *Biochemistry*, *17*, 501–508. <https://doi.org/10.1021/bi00596a020>
- Burakovsky, D. E., Sergiev, P. V., Steblyanko, M. A., Konevega, A. L., Bogdanov, A. A., & Dontsova, O. A. (2011). The structure of helix 89 of 23S rRNA is important for peptidyl transferase function of *Escherichia coli* ribosome. *FEBS Letters*, *585*(19), 3073–3078. <https://doi.org/10.1016/j.febslet.2011.08.030>
- Chadani, Y., Niwa, T., Izumi, T., Sugata, N., Nagao, A., Suzuki, T., ... Taguchi, H. (2017). Intrinsic ribosome destabilization underlies translation and provides an organism with a strategy of environmental sensing. *Molecular Cell*, *68*(3), 528–539.e5. <https://doi.org/10.1016/j.molcel.2017.10.020>
- Charollais, J., Dreyfus, M., & Lost, I. (2004). CsdA, a cold-shock RNA helicase from *Escherichia coli*, is involved in the biogenesis of 50S ribosomal subunit. *Nucleic Acids Research*, *32*(9), 2751–2759. <https://doi.org/10.1093/nar/gkh603>
- Charollais, J., Pflieger, D., Vinh, J., Dreyfus, M., & Lost, I. (2003). The DEAD-box RNA helicase SrmB is involved in the assembly of 50S ribosomal subunits in *Escherichia coli*. *Molecular Microbiology*, *48*(5), 1253–1265. <https://doi.org/10.1046/j.1365-2958.2003.03513.x>
- Chen, S. S., & Williamson, J. R. (2013). Characterization of the ribosome biogenesis landscape in *E. coli* using quantitative mass spectrometry. *Journal of Molecular Biology*, *425*(4), 767–779. <https://doi.org/10.1016/j.jmb.2012.11.040>
- Datsenko, K. A., & Wanner, B. L. (2000). One-step inactivation of chromosomal genes in *Escherichia coli* K-12 using PCR products. *Proceedings of the National Academy of Sciences of the United States of America*, *97*(12), 6640–6645. <https://doi.org/10.1073/pnas.120163297>
- Elles, L. M. S., Sykes, M. T., Williamson, J. R., & Uhlenbeck, O. C. (2009). A dominant negative mutant of the *E. coli* RNA helicase DbpA blocks assembly of the 50S ribosomal subunit. *Nucleic Acids Research*, *37*(19), 6503–6514. <https://doi.org/10.1093/nar/gkp711>
- Fischer, N., Neumann, P., Konevega, A. L., Bock, L. V., Ficner, R., Rodnina, M. V., & Stark, H. (2015). Structure of the *E. coli* ribosome–EF-Tu complex at <3 Å resolution by Cs-corrected cryo-EM. *Nature*, *520*(7548), 567–570. <https://doi.org/10.1038/nature14275>
- Gabriel, S. E., & Helmann, J. D. (2009). Contributions Zur-controlled ribosomal proteins to growth under zinc starvation conditions. *Journal of Bacteriology*, *191*(19), 6116–6122. <https://doi.org/10.1128/JB.00802-09>
- Gilston, B. A., Wang, S., Marcus, M. D., Canalizo-Hernández, M. A., Swindell, E. P., Xue, Y. I., ... O'Halloran, T. V. (2014). Structural and mechanistic basis of zinc regulation across the *E. coli* Zur regulon. *PLoS Biology*, *12*(11), e1001987. <https://doi.org/10.1371/journal.pbio.1001987>
- Graham, A. I., Hunt, S., Stokes, S. L., Bramall, N., Bunch, J., Cox, A. G., ... Poole, R. K. (2009). Severe zinc depletion of *Escherichia coli*: roles for high affinity zinc binding by ZinT, zinc transport and zinc-independent proteins. *Journal of Biological Chemistry*, *284*(27), 18377–18389. <https://doi.org/10.1074/jbc.M109.001503>
- Guzman, L.-M., Belin, D., Carson, M. J., & Beckwith, J. (1995). Tight regulation, modulation, and high-level expression by vectors containing the arabinose P_{BAD} promoter. *Journal of Bacteriology*, *177*(14), 4121–4130. <https://doi.org/10.1128/jb.177.14.4121-4130.1995>
- Hager, J., Staker, B. L., Bugl, H., & Jakob, U. (2002). Active site in RrmJ, a heat shock-induced methyltransferase. *Journal of Biological Chemistry*, *277*(44), 41978–41986. <https://doi.org/10.1074/jbc.M205423200>
- Hantke, K. (2005). Bacterial zinc uptake and regulators. *Current Opinion in Microbiology*, *8*(2), 196–202. <https://doi.org/10.1016/j.mib.2005.02.001>
- Hardy, S. J. (1975). The stoichiometry of the ribosomal proteins of *Escherichia coli*. *Molecular and General Genetics*, *140*(3), 253–274. <https://doi.org/10.1007/BF00334270>
- Hardy, S. J., Kurland, C. G., Voynow, P., & Mora, G. (1969). The ribosomal proteins of *Escherichia coli*. I. Purification of 30S ribosomal proteins. *Biochemistry*, *8*(7), 2897–2905. <https://doi.org/10.1021/bi00835a031>
- Hemm, M. R., Paul, B. J., Miranda-Ríos, J., Zhang, A., Soltanzad, N., & Storz, G. (2010). Small stress response proteins in *Escherichia coli*: Proteins missed by classical proteomic studies. *Journal of Bacteriology*, *192*(1), 46–58. <https://doi.org/10.1128/JB.00872-09>
- Hensley, M. P., Gunasekera, T. S., Easton, J. A., Sigdel, T. K., Sugarbaker, S. A., Klingbeil, L., ... Crowder, M. W. (2012). Characterization of Zn (II)-responsive ribosomal proteins YkgM and L31 in *E. coli*. *Journal of Inorganic Biochemistry*, *111*, 164–172. <https://doi.org/10.1016/j.jinorgbio.2011.11.022>
- Hensley, M. P., Tierney, D. L., & Crowder, M. W. (2011). Zn(II) binding to *Escherichia coli* 70S ribosomes. *Biochemistry*, *50*(46), 9937–9939. <https://doi.org/10.1021/bi200619w>
- Horie, K., Wada, A., & Fukutome, H. (1981). Conformational studies of *Escherichia coli* ribosomes with the use of acridine orange as a probe. *Journal of Biochemistry*, *90*(2), 449–461. <https://doi.org/10.1093/oxfordjournals.jbchem.a133492>
- Ikegami, A., Nishiyama, K., Matsuyama, S., & Tokuda, H. (2005). Disruption of *rpmJ* encoding ribosomal protein L36 decreases the expression of *secY* upstream of the *spc* operon and inhibits protein translocation in *Escherichia coli*. *Bioscience, Biotechnology, and Biochemistry*, *69*, 1595–1602. <https://doi.org/10.1271/bbb.69.1595>
- Iost, I., Bizebard, T., & Dreyfus, M. (2013). Functions of DEAD-box proteins in bacteria: Current knowledge and pending questions. *Biochimica Et Biophysica Acta*, *1829*(8), 866–877. <https://doi.org/10.1016/j.bbagr.2013.01.012>
- Izutsu, K., Wada, A., & Wada, C. (2001). Expression of ribosome modulation factor (RMF) in *Escherichia coli* requires ppGpp. *Genes to Cells*, *6*, 665–676. <https://doi.org/10.1046/j.1365-2443.2001.00457.x>

- Kaczanowska, M., & Rydén-Aulin, M. (2007). Ribosome biogenesis and the translation process in *Escherichia coli*. *Microbiology and Molecular Biology Reviews*, 71(3), 471–494. <https://doi.org/10.1128/MMBR.00013-07>
- Kaltschmidt, E., & Wittmann, H. G. (1970). Ribosomal proteins, XII. Number of proteins in small and large ribosomal subunits of *Escherichia coli* as determined by two-dimensional gel electrophoresis. *Proceedings of the National Academy of Sciences of the United States of America*, 67(3), 1276–1282. <https://doi.org/10.1073/pnas.67.3.1276>
- Katayama, A., Tsujii, A., Wada, A., Nishino, T., & Ishihama, A. (2002). Systematic search for zinc-binding proteins in *Escherichia coli*. *European Journal of Biochemistry*, 269, 2403–2413. <https://doi.org/10.1046/j.1432-1033.2002.02900.x>
- Kato, T., Yoshida, H., Miyata, T., Maki, Y., Wada, A., & Namba, K. (2010). Structure of the 100S ribosome in the hibernation stage revealed by electron cryomicroscopy. *Structure*, 18(6), 719–724. <https://doi.org/10.1016/j.str.2010.02.017>
- Kitagawa, M., Ara, T., Ariuzzaman, M., Ioka-Nakamichi, T., Inamoto, E., Toyonaga, H., & Mori, H. (2005). Complete set of ORF clones of *Escherichia coli* ASKA library (a complete set of *E. coli* K-12 ORF archive): Unique resources for biological research. *DNA Research*, 12(5), 291–299. <https://doi.org/10.1093/dnares/dsi012>
- Leppik, M., Liiv, A., & Remme, J. (2017). Random pseudouridylation in vivo reveals critical region of *Escherichia coli* 23S rRNA for ribosome assembly. *Nucleic Acids Research*, 45(10), 6098–6108. <https://doi.org/10.1093/nar/gkx160>
- Li, Y., Qiu, Y., Gao, H. E., Guo, Z., Han, Y., Song, Y., ... Yang, R. (2009). Characterization of Zur-dependent genes and direct Zur targets in *Yersinia pestis*. *BMC Microbiology*, 9(128), 1–13. <https://doi.org/10.1186/1471-2180-9-128>
- Lilleorg, S., Reier, K., Pulk, A., Liiv, A., Tammsalu, T., Peil, L., ... Remme, J. (2019). Bacterial ribosome heterogeneity: Changes in ribosomal protein composition during transition into stationary growth phase. *Biochimie*, 156, 169–180. <https://doi.org/10.1016/j.biochi.2018.10.013>
- Liu, Q., & Fredrick, K. (2016). Intersubunit bridges of the bacterial ribosome. *Journal of Molecular Biology*, 428(10 Pt B), 2146–2164. <https://doi.org/10.1016/j.jmb.2016.02.009>
- Maeder, C., & Draper, D. E. (2005). A small protein unique to bacteria organizes rRNA tertiary structure over an extensive region of the 50S ribosomal subunit. *Journal of Molecular Biology*, 354(2), 436–446. <https://doi.org/10.1016/j.jmb.2005.09.072>
- Makarova, K. S., Ponomarev, V. A., & Koonin, E. V. (2001). Two C or not two C: Recurrent disruption of Zn-ribbons, gene duplication, lineage-specific gene loss, and horizontal gene transfer in evolution of bacterial ribosomal proteins. *Genome Biology*, 2(9), 1–14. <https://doi.org/10.1186/gb-2001-2-9-research0033>
- Maki, Y., Yoshida, H., & Wada, A. (2000). Two proteins, YfiA and YhbH, associated with resting ribosomes in stationary phase *Escherichia coli*. *Genes to Cells*, 5–12, 965–974. <https://doi.org/10.1046/j.1365-2443.2000.00389.x>
- Mikhaylina, A., Ksibe, A. Z., Scanlan, D. J., & Blindauer, C. A. (2018). Bacterial zinc uptake regulator proteins and their regulons. *Biochemical Society Transactions*, 46(4), 983–1001. <https://doi.org/10.1042/BST20170228>
- Nanamiya, H., Akanuma, G., Natori, Y., Murayama, R., Kosono, S., Kudo, T., ... Kawamura, F. (2004). Zinc is a key factor in controlling alternation of two types of L31 protein in the *Bacillus subtilis* ribosomes. *Molecular Microbiology*, 52(1), 273–283. <https://doi.org/10.1111/j.1365-2958.2003.03972.x>
- Noll, M., Hapke, B., Schreire, M. H., & Noll, H. (1973). Structural dynamics of bacterial ribosomes. I. Characterization of vacant couples and their relation to complexed ribosomes. *Journal of Molecular Biology*, 75(2), 281–294.
- Ortiz, J. O., Brandt, F., Matias, V. R. F., Sennels, L., Rappsilber, J., Scheres, S. H. W., ... Baumeister, W. (2010). Structure of hibernating ribosomes studied by cryoelectron tomography in vitro and in situ. *Journal of Cell Biology*, 190, 4613–4621. <https://doi.org/10.1083/jcb.201005007>
- Owen, G. A., Pascoe, B., Kallifidas, D., & Paget, M. S. (2007). Zinc-responsive regulation of alternative ribosomal protein genes in *Streptomyces coelicolor* involves Zur and σ^R . *Journal of Bacteriology*, 189(11), 4078–4086. <https://doi.org/10.1128/JB.01901-06>
- Panina, E. M., Mironov, A. A., & Gelfand, M. S. (2003). Comparative genomics of bacterial zinc regulons: Enhanced ion transport, pathogenesis, and rearrangement of ribosomal proteins. *Proceedings of the National Academy of Sciences of the United States of America*, 100(17), 9912–9917. <https://doi.org/10.1073/pnas.1733691100>
- Patzer, S. I., & Hantke, K. (2000). The zinc-responsive regulator Zur and its control of the *znu* gene cluster encoding the ZnuABC zinc uptake system in *Escherichia coli*. *Journal of Biological Chemistry*, 275(32), 24321–24332. <https://doi.org/10.1074/jbc.M001775200>
- Shajani, Z., Sykes, M. T., & Williamson, J. R. (2011). Assembly of bacterial ribosomes. *Annual Review of Biochemistry*, 80, 501–526. <https://doi.org/10.1146/annurev-biochem-062608-160432>
- Shasmal, M., Chakraborty, B., & Sengupta, J. (2010). Intrinsic molecular properties of the protein-protein bridge facilitate ratchet-like motion of the ribosome. *Biochemical and Biophysical Research Communications*, 399(2), 192–197. <https://doi.org/10.1016/j.bbrc.2010.07.053>
- Shimada, T., Yoshida, H., & Ishihama, A. (2013). Involvement of cyclic AMP receptor protein in regulation of the *rmf* gene encoding the ribosome modulation factor in *Escherichia coli*. *Journal of Bacteriology*, 195, 2212–2219. <https://doi.org/10.1128/JB.02279-12>
- Shimizu, Y., Kanamori, T., & Ueda, T. (2005). Protein synthesis by pure translation systems. *Methods*, 36(3), 299–304. <https://doi.org/10.1016/j.ymeth.2005.04.006>
- Shimizu, Y., & Ueda, T. (2010). PURE technology. *Methods in Molecular Biology*, 607, 11–21. https://doi.org/10.1007/978-1-60327-331-2_2
- Shin, J. H., & Helmann, J. D. (2016). Molecular logic of the Zur-regulated zinc deprivation response in *Bacillus subtilis*. *Nature Communications*, 7, 12612. <https://doi.org/10.1038/ncomms12612>
- Tal, M., Weissman, I., & Silberstein, A. (1990). A new method for stoichiometric analysis of proteins in complex mixture—reevaluation of the stoichiometry of *E. coli* ribosomal proteins. *Journal of Biochemical and Biophysical Methods*, 21(3), 247–266.
- Ueta, M., Ohniwa, R. L., Yoshida, H., Maki, Y., Wada, C., & Wada, A. (2008). Role of HPF (Hibernation Promoting Factor) in translational activity in *Escherichia coli*. *Journal of Biochemistry*, 143(3), 425–433. <https://doi.org/10.1093/jb/mvm243>
- Ueta, M., Wada, C., Bessho, Y., Maeda, M., & Wada, A. (2017). Ribosomal protein L31 in *Escherichia coli* contributes to ribosome subunit association and translation, whereas short L31 cleaved by protease 7 reduces both activities. *Genes to Cells*, 22(5), 452–471. <https://doi.org/10.1111/gtc.12488>

- Ueta, M., Wada, C., Daifuku, T., Sako, Y., Bessho, Y., Kitamura, A., ... Wada, A. (2013). Conservation of two distinct types of 100S ribosome in bacteria. *Genes to Cells*, 18(7), 554–574. <https://doi.org/10.1111/gtc.12057>
- Ueta, M., Wada, C., & Wada, A. (2010). Formation of 100S ribosomes in *Staphylococcus aureus* by the hibernation promoting factor homolog SaHPF. *Genes to Cells*, 15, 43–58. <https://doi.org/10.1111/j.1365-2443.2009.01364.x>
- Ueta, M., Yoshida, H., Wada, C., Baba, T., Mori, H., & Wada, A. (2005). Ribosome binding proteins YfiA and YhbH have opposite functions during 100S formation in the stationary phase of *Escherichia coli*. *Genes to Cells*, 10(12), 1103–1112. <https://doi.org/10.1111/j.1365-2443.2005.00903.x>
- Urlaub, H., Kruff, V., Bischof, O., Müller, E. C., & Wittmann-Liebold, B. (1995). Protein-rRNA binding features and their structural and functional implications in ribosomes as determined by cross-linking studies. *EMBO Journal*, 14(18), 4578–4588. <https://doi.org/10.1002/j.1460-2075.1995.tb00137.x>
- Velasco, E., Wang, S., Sanet, M., Fernández-Vázquez, J., Jové, D., Glaria, E., ... Balsalobre, C. (2018). A new role for Zinc limitation in bacterial pathogenicity: Modulation of α -hemolysin from uropathogenic *Escherichia coli*. *Scientific Reports*, 8(1), 6535–6546. <https://doi.org/10.1038/s41598-018-24964-1>
- Wada, A. (1986a). Analysis of *Escherichia coli* ribosomal proteins by an improved two dimensional gel electrophoresis. I. Detection of four new proteins. *Journal of Biochemistry*, 100(6), 1583–1594. <https://doi.org/10.1093/oxfordjournals.jbchem.a121866>
- Wada, A. (1986b). Analysis of *Escherichia coli* ribosomal proteins by an improved two dimensional gel electrophoresis. II. Characterization of four new proteins. *Journal of Biochemistry*, 100(6), 1595–1605. <https://doi.org/10.1093/oxfordjournals.jbchem.a121867>
- Wada, A. (1998). Growth phase coupled modulation of *Escherichia coli* ribosomes. *Genes to Cells*, 3(4), 203–208.
- Wada, A., Igarashi, K., Yoshimura, S., Aimoto, S., & Ishihama, A. (1995). Ribosome modulation factor: Stationary growth phase-specific inhibitor of ribosome functions from *Escherichia coli*. *Biochemical and Biophysical Research Communications*, 214(2), 410–417. <https://doi.org/10.1006/bbrc.1995.2302>
- Wada, A., & Sako, T. (1987). Primary Structures of and Genes for New Ribosomal proteins A and B in *Escherichia coli*. *Journal of Biochemistry*, 101(3), 817–820. <https://doi.org/10.1093/jb/101.3.817>
- Wada, A., Yamazaki, Y., Fujita, N., & Ishihama, A. (1990). Structure and probable genetic location of a “ribosome modulation factor” associated with 100S ribosomes in stationary-phase *Escherichia coli* cells. *Proceedings of the National Academy of Sciences of the United States of America*, 87(7), 2657–2661. <https://doi.org/10.1073/pnas.87.7.2657>
- Yoshida, H., Maki, Y., Kato, H., Fujisawa, H., Izutsu, K., Wada, C., & Wada, A. (2002). The ribosome modulation factor (RMF) binding site on the 100S ribosome of *Escherichia coli*. *Journal of Biochemistry*, 132(6), 983–989. <https://doi.org/10.1093/oxfordjournals.jbchem.a003313>
- Yoshida, H., & Wada, A. (2014). The 100S ribosome: Ribosomal hibernation induced by stress. *Wiley Interdisciplinary Reviews: RNA*, 5(5), 723–732. <https://doi.org/10.1002/wrna.1242>
- Yoshida, H., Yamamoto, H., Uchiumi, T., & Wada, A. (2004). RMF inactivates ribosomes by covering the peptidyl transferase centre and entrance of peptide exit tunnel. *Genes to Cells*, 9, 271–278. <https://doi.org/10.1111/j.1356-9597.2004.00723.x>

SUPPORTING INFORMATION

Additional supporting information may be found online in the Supporting Information section.

How to cite this article: Ueta M, Wada C, Wada A. YkgM and YkgO maintain translation by replacing their paralogs, zinc-binding ribosomal proteins L31 and L36, with identical activities. *Genes Cells*. 2020;25:562–581. <https://doi.org/10.1111/gtc.12796>